6-2020

Prototype System for Implementing the Ultrasonic Guided Wave Method on the Field

Ece Erdogmus
University of Nebraska-Lincoln, eerdogmus@unl.edu

Eric Garcia
University of Nebraska - Lincoln

Michael Schuller
University of Nebraska - Lincoln

Ahmad Shoaib Amiri
University of Nebraska - Lincoln, shoaib7amiri@gmail.com

PROTOTYPE SYSTEM FOR IMPLEMENTING THE ULTRASONIC GUIDED WAVE METHOD ON THE FIELD

PI: Ece Erdogmus, Ph.D., P.E.

Research Team

Eric Garcia, Ph.D.; Michael Schuller, P.E.; Shoaib Amiri

FINAL REPORT

Durham School of Architectural Engineering and Construction

1110 South 67 Street, Omaha, NE 68182

Sponsored By

Nebraska Department of Transportation and U.S. Department of Transportation Federal Highway Administration

August 2020

NEBRASKA
Good Life. Great Journey.
DEPARTMENT OF TRANSPORTATION

THE DURHAM SCHOOL
OF ARCHITECTURAL ENGINEERING AND CONSTRUCTION

TECHNICAL REPORT DOCUMENTATION PAGE

To add text, click inside the form field below (will appear as a blue highlighted or outlined box) and begin typing. The instructions will be replaced by the new text. Only boxes with form fields must be completed.

Please remove this field before completing form.

1. Report No. M086	**2. Government Accession No.** NA	**3. Recipient's Catalog No.**
4. Title and Subtitle Prototype System for Implementing the Ultrasonic Guided Wave Method on the Field		**5. Report Date** June 2020 **6. Performing Organization Code** NA
7. Author(s) Ece Erdogmus, PhD, PE; Eric Garcia, PhD; Michael Schuller, PE; Shoaib Amiri		**8. Performing Organization Report No.** NA
9. Performing Organization Name and Address Durham School of Architectural Engineering and Construction University of Nebraska-Lincoln 107 Peter Kiewit Institute (PKI) 1110 S. 67th Street Omaha, NE 68182		**10. Work Unit No.** **11. Contract** SPR-P1(19) M086
12. Sponsoring Agency Name and Address Nebraska Department of Transportation Research Section 1400 Hwy 2 Lincoln, NE 68502		**13. Type of Report and Period Covered** Final Report July 2018-June 2020 **14. Sponsoring Agency Code**

15. Supplementary Notes

If applicable, enter information not included elsewhere, such as translation of (or by), report supersedes, old edition number, alternate title (e.g. project name), or hypertext links to documents or related information.

16. Abstract

This report presents the latest improvements in a recently developed nondestructive testing (NDT) technique for early detection of various flaws such as corrosion, delamination, and concrete cracking in reinforced concrete (RC) bridge decks. The method, named Ultrasonic Guided Wave Leakage (UGWL) method by the developing authors, involves use of internal steel reinforcement (rebar) as a wave guide for transmitting ultrasonic waves through the system and the measurement of leaked energy at the surface of the concrete. This report builds upon the progress made in the previously published phases of the project (M029 and M066), and aims to further explore the capabilities and practicality of the proposed NDT method. Specifically, efficient coupling of the sensors to the reinforcement and to concrete, durable embedment of sensors in field conditions, detection of corrosion development, benchmarking with half-cell potential (HCP) and chloride level tests, and suggestions for optimal sensor arrays are explored via laboratory and field testing. Results show that with careful placement of sensors and data interpretation, onset and progression of localized corrosion can be detected, which will be useful in developing deterioration models for RC bridge decks in the future. Results show that the UGWL results match well with chloride level tests and HCP testing predictions for potential for corrosion. For field applications, an angled seat made of fast-setting Hydrocal gypsum cement is recommended and it is projected that the optimal angle of attachment is 33 degrees or less from the vertical axis.

17. Key Words	**18. Distribution Statement**
Nondestructive tests, corrosion tests, corrosion, reinforced concrete bridges, ultrasonic tests, ultrasonic waves	No restrictions. This document is available through the National Technical Information Service. 5285 Port Royal Road Springfield, VA 22161

19. Security Classification (of this report)	**20. Security Classification (of this page)**	40	**22. Price**
Unclassified	Unclassified		

Form DOT F 1700.7 (8-72) Reproduction of completed page authorized

DISCLAIMER

The contents of this report reflect the views of the authors, who are responsible for the facts and the accuracy of the information presented herein. The contents do not necessarily reflect the official views or policies neither of the Nebraska Department of Transportations nor the University of Nebraska-Lincoln. This report does not constitute a standard, specification, or regulation. Trade or manufacturers' names, which may appear in this report, are cited only because they are considered essential to the objectives of the report.

The United States (U.S.) government and the State of Nebraska do not endorse products or manufacturers. This material is based upon work supported by the Federal Highway Administration under SPR-P1(19) M086. Any opinions, findings and conclusions or recommendations expressed in this publication are those of the author(s) and do not necessarily reflect the views of the Federal Highway Administration."

Contents

Prototype System for Implementing the Ultrasonic Guided Wave Method on the Field

Authors: Ece Erdogmus, PhD, PE; Eric Garcia, PhD; Mike Schuller, PE; Shoaib Amiri

Abstract

This report presents the latest improvements in a recently developed nondestructive testing (NDT) technique for early detection of various flaws such as corrosion, delamination, and concrete cracking in reinforced concrete (RC) bridge decks. The method, named Ultrasonic Guided Wave Leakage (UGWL) method by the developing authors, involves use of internal steel reinforcement (rebar) as a wave guide for transmitting ultrasonic waves through the system and the measurement of leaked energy at the surface of the concrete. This report builds upon the progress made in the previously published phases of the project (M029 and M066), and aims to further explore the capabilities and practicality of the proposed NDT method. Specifically, efficient coupling of the sensors to the reinforcement and to concrete, durable embedment of sensors in field conditions, detection of corrosion development, benchmarking with half-cell potential (HCP) and chloride level tests, and suggestions for optimal sensor arrays are explored via laboratory and field testing. Results show that with careful placement of sensors and data interpretation, onset and progression of localized corrosion can be detected, which will be useful in developing deterioration models for RC bridge decks in the future. Results show that the UGWL results match well with chloride level tests and HCP testing predictions for potential for corrosion. For field applications, an angled seat made of fast-setting Hydrocal gypsum cement is recommended and it is projected that the optimal angle of attachment is 33 degrees or less from the vertical axis.

1. Introduction

This report presents the most recent findings on the implementatation of the recently developed Ultrasonic Guided Wave Leakage (UGWL) method in the field. The ultimate goal of the larger study is to develop a novel nondestructive testing (NDT) method for the continuous health monitoring of reinforced concrete bridge decks (new or recently replaced) to identify the onset and progression of various flaws: corrosion, delamination, and concrete cracking.

The method, named Ultrasonic Guided Wave Leakage (UGWL) method by the developing authors, involves use of internal steel reinforcement (rebar) as a wave guide for transmitting ultrasonic waves through the system and the measurement of leaked energy at the surface of the concrete. The results are processed in the frequency domain and amplitude measurements are utilized for the detection of changes in the system. This report builds upon the progress made in the previously published phases of the project (M029 and M066), and aims to further explore the capabilities and practicality of the proposed NDT method.

In the previously published phases of this study, first, the proof of concept for the proposed UGWL method's ability to detect the onset of delamination in reinforced concrete was demonstrated successfully, where a delamination between the rebar and the concrete as small as 0.008 in could be detected (Garcia et al., 2017). Then, early detection of the onset of corrosion and cracking in concrete was also demonstrated in simple concrete slabs with unidirectional reinforcement (Garcia et al., 2019). Later, in project M066, the effect of bidirectional reinforcement and longer propagation distances up to 10 ft were investigated experimentally in the lab, as well as a pilot field implementation (Erdogmus et al., 2020).

In this particular project, efficient coupling of the sensors to the reinforcement and to concrete, durable embedment of sensors in field conditions, detection of corrosion development, benchmarking with half-cell potential (HCP) and chloride level tests, and suggestions for optimal sensor arrays are explored via laboratory and field testing. This report also aims to demonstrate that the recently developed UGWL technique has several advantages over the commonly used Half-Cell Potential (HCP) method in the detection of corrosion in reinforced concrete (RC) bridge decks.

Specific objectives of the project are as follows:

1. To develop a suitable attachment for the transmitter to the rebar
2. To evaluate the system hardness and durability in the field in terms of adhesives/attachments as well as the effect of vehicular vibration/impact
3. To develop recommendations for the location of the transmitter and receivers on actual bridge decks
    - What are the best locations for the transmitter for common issues?
    - What are the best locations for an array of receivers for common issues?
4. To validate the results and benchmark the method on the field
5. *To demonstrate that the recently developed UGWL technique has several advantages over the commonly used Half-Cell Potential (HCP) method in the detection of corrosion in reinforced concrete (RC) bridge decks
6. *To quantify the level of damage detected by UGWL data via chloride level measurements

*These two objectives were not in the initial project scope, however, through discussions with the Technical Advisory Committee (TAC), we included these objectives in our work as the project progressed.

To achieve these objectives, laboratory experiments, field work, as well as a pros-and-cons analysis between UGWL and HCP are performed. Finally, a quantitative correlation between UGWL data and chloride threshold levels (CTLs) is explored.

2. Background

This study is motivated by the increased demand for structural health monitoring (SHM) systems for the rapidly aging U.S. infrastructure. According to literature, more than half of the bridges in the United States are made up of reinforced concrete (Hartt et al., 2004). Reinforced concrete structures are succeptible to problems caused by corrosion, delamination, and cracking, which may adversely influence the integrity and structural capacity of the composite structure. Reinforced concrete bridge decks are particularly vulnerable to corrosion and delamination because of the harsh conditions they commonly undergo including freeze-thaw cycles, de-icing salts, continuous impact from heavy traffic, and exposure to water. As of 2015, the National Bridge Inventory (NBI) states that 142,915 out of the 611,845 highway bridges in the United States, or approximately 23 percent, are structurally deficient (FHWA, 2014a). Research shows that the annual corrosion related repair costs for highway bridges exceeds $8.3 billion. This includes $2 billion for bridge deck repairs (Cui, 2012), with corrosion and delamination accounting for almost 40 percent of these costs (Yunovich et al., 2001).

Corrosion can result in delamination when left unmanaged. As explained in more detail in Garcia et al. (2019), chemical delamination forms the first phase of corrosion-related deterioration. These initial phases of corrosion temporarily strenghthen the concrete-steel bond. As corrosion develops, formation of iron oxides at the steel surface leads to significant volumetric increase. This in turn produces internal pressures at the steel-concrete interface, and once the internal pressures cause the concrete to experience great enough tensile stresses, mechanical delamination is experienced.

Ultrasonic Guided Wave Leakage (UGWL) Method

Many studies show that in general, ultrasonic testing (UT) methods provide small enough wavelengths that they can be utilized for detection of smaller flaws than other NDT methods, such as ground penetrating radar or impact echo. The recently-developed UGWL method further improves the applicability of UT-based methods by utilizing the steel as the waveguide and the leaked energy into the surrounding concrete is measured using an array of sensors. In the previous phases of this project, it was successfully demonstrated that this method can be used to detect the onset of various flaws such as corrosion, delamination, and cracking. It was successfully demonstrated that the proposed technique has the potential to identify the onset of delamination as small as 0.008 inches. Previous work also showed promise for detection of the progression of corrosion in lab conditions for 40 days using slabs cast with and submerged under 5% NaCl solution as shown in Figure 1. Further, based on the lab measurements the leaked energy could be detected effectively using a single transmitter as far as 10 feet from the transmitter. Details of these previous findings can be found in NDOT final project reports for project numbers M029 and M066, as well as Garcia et al. 2017 and 2019.

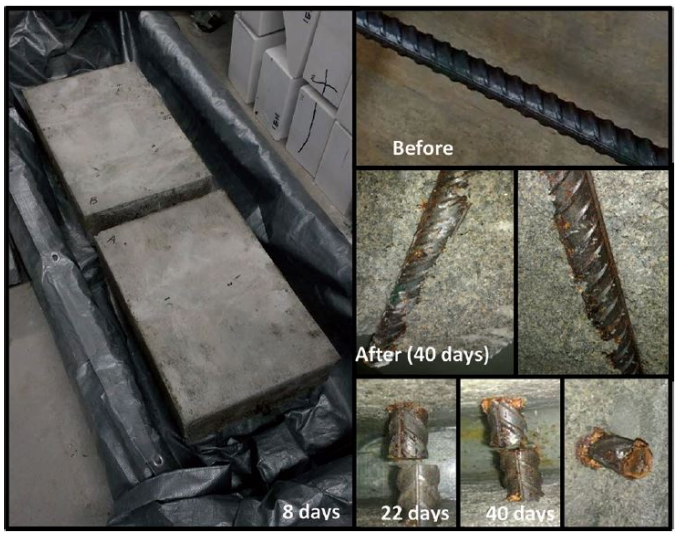

Figure 1. Corrosion specimens (Garcia et al., 2019)

One of the key concepts of this method is that the amplitudes of ultrasonic energy leaked from the rebar are sensitive to the type of flaw in the rebar, concrete, or the rebar-concrete interface. For instance, the amplitudes of leaked ultrasonic energy into the surrounding concrete increase when the bond between the concrete and steel improve during the initial phases of corrosion material build up (Figure 2). Figure 2 also shows that while the change can also be observed in velocity readings (graph on top), the change is more pronounced and easier to detect in the amplitude readings in the frequency domain (bottom image).

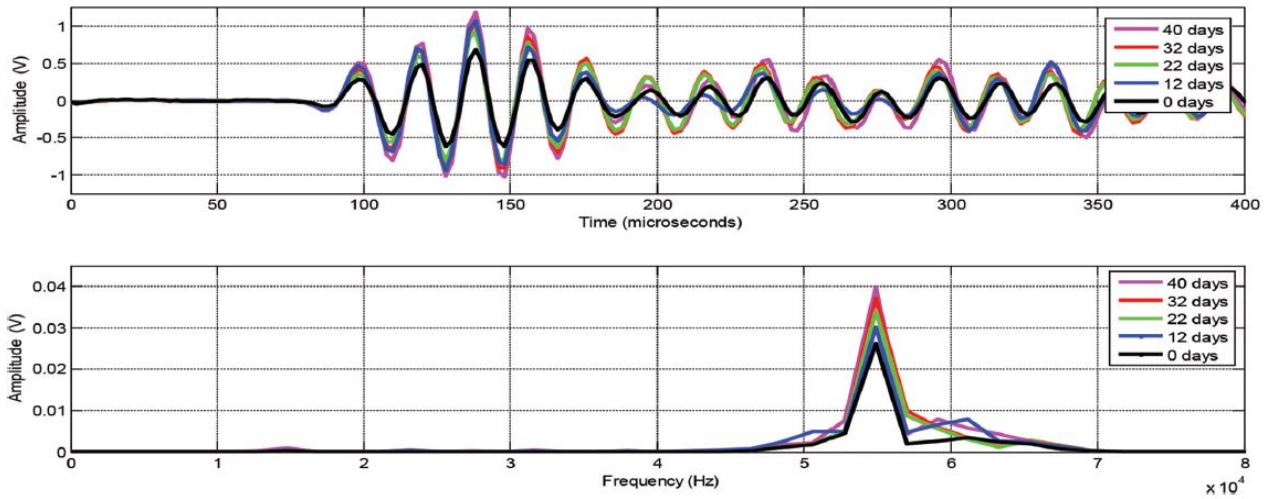

Figure 2. Amplitude measurements indicating corrosion progression (Garcia et al., 2019)

After the initial phase of corrosion buildup, the tensile stresses can cause delamination between the concrete and the steel. In the case of a delamination, the amplitude readings of the leaked energy over the delamination area is expected to decrease as confirmed in previous phases of the study looking at delamination. Once the delamination area is passed, the amplitudes would then again increase as more energy was maintained in the wave guide (rebar) to leak into the concrete after the delam region. This

evolving nature of the bond between the steel and concrete, and the UGWL method's sensitivity to it, presents one of the unique features of the proposed technique, which has the capability to capture the entire RC bridge deck deterioration progression. This knowledge can, in turn, help update bridge deck deterioration models used by DOTs and inform design, maintenance, and repair processes for reinforced concrete bridge decks. As such, the method has the potential to help decrease the large economic burdens on the states that are caused by corrosion and delamination related repairs.

Half-Cell Potential Method

In order to benchmark the results of the new method (UGWL) to another method that is well-known, the Half-Cell Potential (HCP) technique is also used to monitor the progression of corrosion activity in the submerged specimens. HCP is a rapid and cost-effective *in situ* testing procedure. ASTM C876 (1999) provides guidance on how to conduct the HCP measurements and how to interpret readings. The relationship between the potential measurements and the probability for corrosion activity is shown in shown in Table 1. In general, the absolute value of the HCP readings increase as the potential of corrosion increases.

Table 1. ASTM C876 for interpretation of HCP measurements

Half-cell potential measurements (mV)	Probability of rebar corrosion activity
>-200	Less than 10%
-200 to -350	Uncertain
<-350	Greater than 90%

HCP method is a relatively easy testing procedure and therefore it used commonly for corrosion testing in bridge decks. However, there are some limitations associated with this technique. One of the disadvantages of the HCP method is that there is a large range of readings between –200 and –350 mV that provide no definitive or quantitative information regarding corrosion potential. Another limitation of HCP method is that it is not suitable for measurements involving epoxy-coated steel as explicitly stated in the ASTM C876 standard.

Chloride Content Analysis

Corrosion is initiated once the chloride content present in the concrete exceeds a certain threshold, called the chloride threshold level (CTL). This threshold value is also referred to as critical chloride content in literature. CTL is often expressed in terms of chloride content relative to the weight of the cement (Angst et al., 2009). Another method to indicate chloride content that is used by researchers is to express CTL as a ratio of free chloride to hydroxyl threshold or $[Cl^-]:[OH^-]$ (Ann & Song, 2007; Angst et al., 2009; Glass & Buenfeld, 2000). Different standards provide guidance on CTL in concrete. For instance, Technology in Practice (*TIP*) by National Ready Mix Concrete Association (NRMCA) suggests that the CTL in concrete is in the range of 0.05 to 0.1% by weight of **concrete**. Table 2 lists the CTLs provided by other standards, expressed in terms of chloride content relative to percentage weight of the **cement**.

Table 2. Chloride threshold values specified by different standards

Standard	Reference	Chloride Threshold Level (CTL) (%, cement)		
		Reinforced Concrete		Pre-stressed Concrete
British Standard	Standard (1997)	0.4	N/A	0.1
ACI 357 (Water-soluble Cl^-)	ACI 357 (1984)	0.1	0.9	0.06
ASTM 1152 (Acid-soluble Cl^-)	ASTM (2012)	0.2	1.2	0.08

In this project, the appropriate CTL limits from Table 2 will be considered to quantify the level of corrosion activity detected by the UGWL readings.

3. Lab experiments

Two sets of lab experiments were conducted in the Structures Laboratory of the University of Nebraska-Lincoln located in the Peter Kiewit Institute (PKI) of Omaha (Scott) Campus. The details on these experimental procedures are given as follows:

3.1 Specimen Set 1

Specimen Set 1 consisted of three reinforced concrete slabs that each measured 36 x 18 x 5 inch as shown in Figure 3. These slabs were cast with a number 4 rebar embedded at the center of the slab cross-section. The rebar was projected at both ends, so that a transmitter could be attached to the end of the rebar to generate the guided waves.

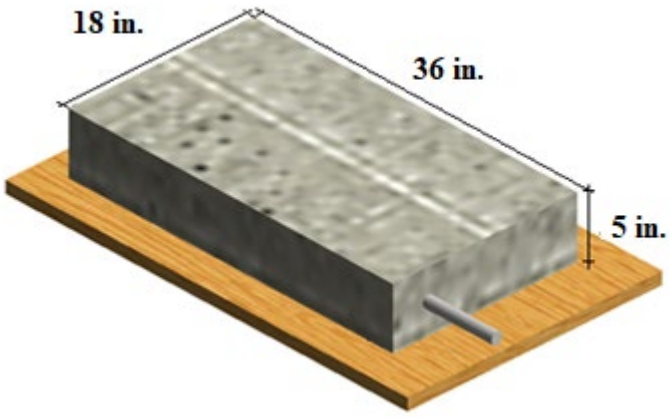

Figure 3. Lab specimens

The concrete mix design (47BD) provided in Table 3 was used to cast the specimens. This mix is generally used by Nebraska Department of Transportation (NDOT) for bridge decks.

Table 3. Properties of NDOT 47BD Mix Design used to cast the lab specimens

Designation	Total Cementitious Material Min. (lb/cy)	Total Aggregate (lb/cy)	Air Content range (%)	Maximum Water/ Cement Ratio (lb/lb)	Minimum Required Strength (psi)
AASHTO Bridge Specification	611	2500-3000	6±1.5	0.49	4000
47BD NDOT	658	2500-3000	6.0-8.5	0.42	4000

The objectives of this set of specimens were as follows:

(1) To investigate energy transmission efficiency with different bar end angles: 0-degree; 33-degree; and 45-degree, cut with reference to vertical axis to simulate different transmitter to rebar attachment seat angles from top of the bar (Figure 4);

(2) To compare two couplants to improve the coupling of the sensors to the test materials: Ultragel II from Magnaflux and White Lithium Grease from Lucas Oil Products;

(3) To monitor the corrosion activity in test specimens using both the UGWL and HCP methods;

(4) To establish a quantitative correlation between UGWL data and chloride content in the test specimens.

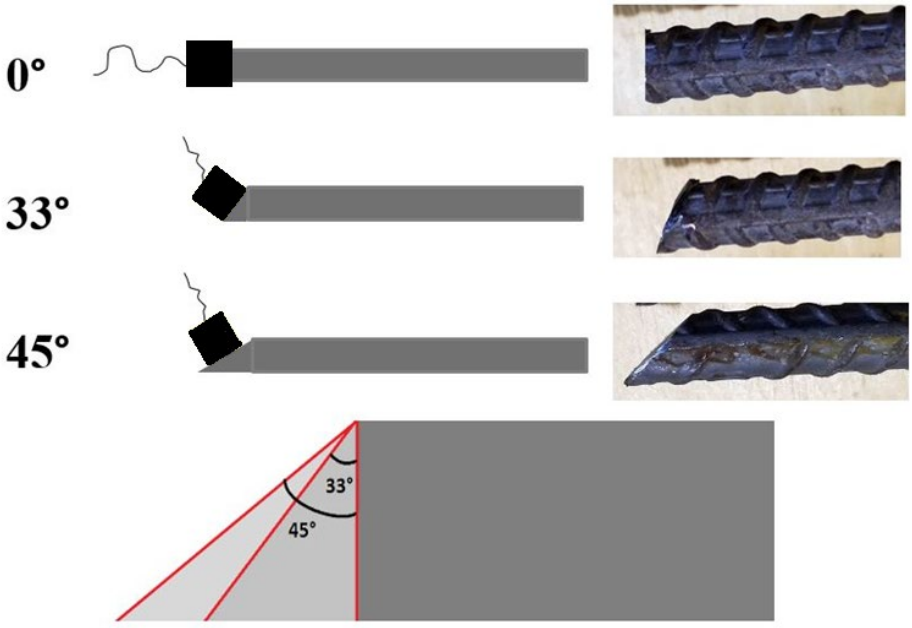

Figure 4. Bar end angles used in Specimen Set 1

To perform the ultrasonic measurements, the PULSONIC Ultrasonic Pulse Analyzer 58-E4900 from CONTROLS-Group is used, and the typical experimental set up for the novel UGWL method is illustrated in Figures 5 and 6. In this method, a transmitter is attached to one end of the rebar to transmit ultrasonic pulses longitudinally. The ultrasonic waves propagate trough the steel reinforcement, which acts as a waveguide. Part of the energy gets leaked out of the rebar and propagate through the surrounding materials, which is concrete in this case. The leaked energy is monitored using an array of receivers located on the concrete surface, as demonstrated in Figure 6.

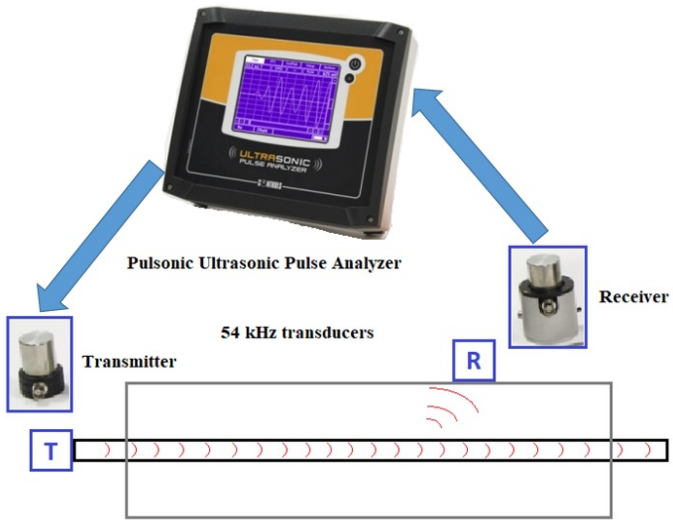

Figure 5. Experimental set-up for UGWL testing procedure

Figure 6. Experimental setup illustrated on one of the Specimen Set 3 slabs

Giatech iCOR was used to collect the HCP measurements. The experimental set-up for this testing procedure is shown in Figure 7, where 'I' shows the location of iCOR device on different spots on the concrete surface, and 'R' shows the reference electrode that is attached to the rebar. This device is

comprised of six corrosion measurement electrodes, one half-cell potential measurement electrode, and one temperature measurement inlet. The equipment is connected to a mobile device such as a tablet via Bluetooth, where the collected data are directly stored.

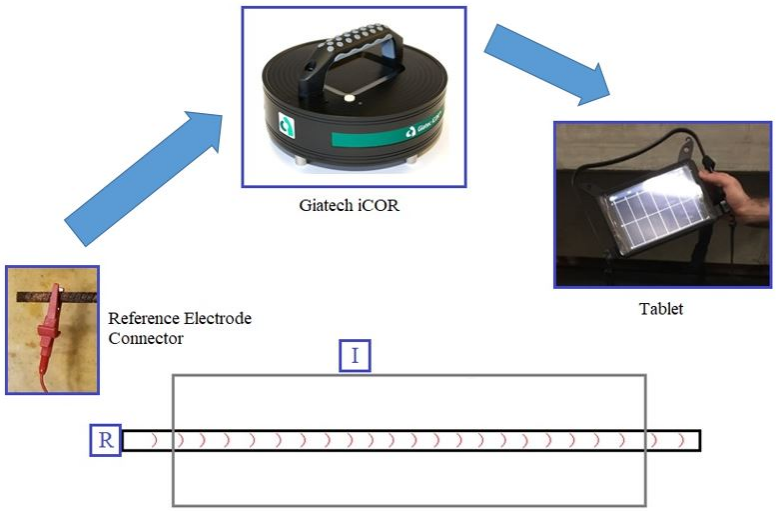

Figure 7. Experimental set-up for HCP measurements

For collection of ultrasonic data using UGWL method, ten equally-spaced spots were marked on the concrete surface of the specimens. These test locations were 3 inches apart, with the first spot starting at 6 inches from the edge of the slab as shown in Figure 8 (a). For collection of HCP measurements, 5 spots that were 6 inches apart were marked as shown in Figure 8 (b). The measurements were taken once every 3 days for the first 30 days and every 6 days for the rest of the process, up to 175 days. Data collected from UGWL technique are analyzed in the frequency domain and the change in the amplitude values are recorded. An increase in these values can be correlated to increased corrosion activity in the region corresponding to the increased amplitudes in the test specimen as the initial stage of corrosion improves the bond between concrete and steel thus increasing the amount of leaked energy.

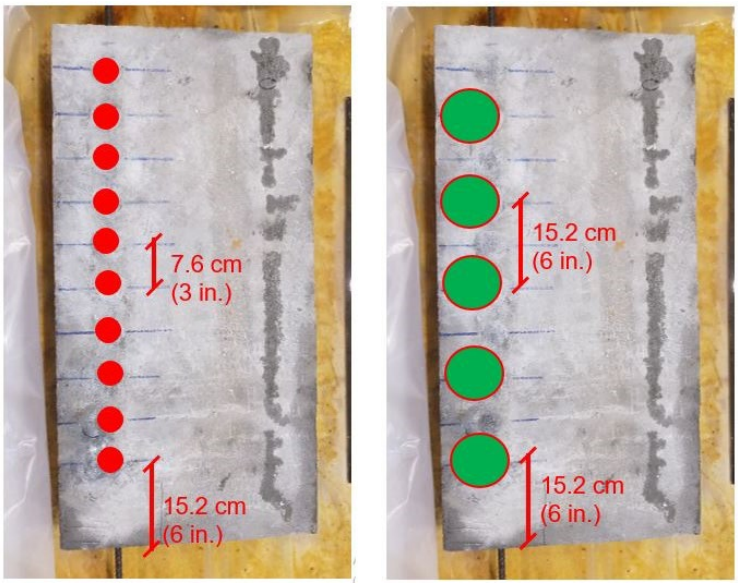

(a) (b)

Figure 8. Test locations on the specimens: (a) UGW; (b) HCP

3.1.1 Results of Specimen Set 1: Effect of Bar End Angles

One of the objectives of these specimens was to investigate the amount of energy transfer with different bar end angles, in order to determine a feasible angle to attach a sensor to a rebar from the top with an angled seat while still achieving the guided wave phenomenon to a reasonable degree. For this purpose, the ends of the rebar are cut at 0, 33, and 45-degrees (as shown in Figure 4) to simulate angled sensor to rebar attachment scenarios. Figure 9 shows the data plots obtained for these three specimens with different bar end angles and each data set's fit to an exponential curve.

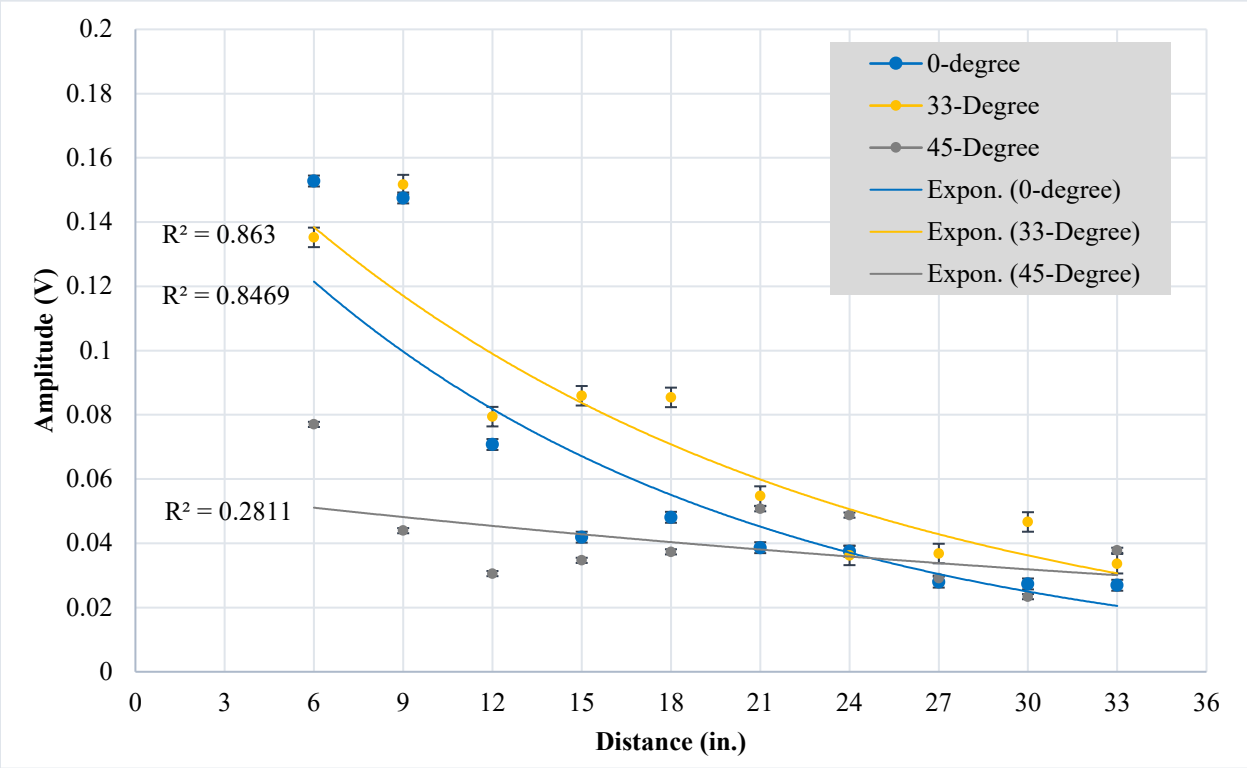

Figure 9. Comparison of the UGWL data for the 0-, 33-, and 45-degree specimens

This comparison points out the following: as expected, maximum energy transfer was obtained from the 0-degree specimen with a peak amplitude around 0.15 V. The 33-degree specimen provided not only comparable peak amplitudes (around 0.14 V), but also a comparable fit to an exponential decay, despite the fact that additional modes of ultrasonic waves were excited that lead to reflections of the leaked energy from the boundaries of the wave guide. In the case of the 45-degree specimen, much less energy was transmitted longitudinally that resulted in significantly lower amplitudes detected from the concrete surface along the array. Also a very low level of correlation to the exponential curve is observed with the 45-degree specimen. Given the significant loss of energy and lack of data reliability in this setup; it was concluded that a 45-degree angle of attachment is infeasible for field applications. It was observed that 33-degree angle attachment appear to be optimal among the tested angles, representing a compromise between a feasible attachment on a horizontal rebar and maintaining most of the energy longitudinally in the wave guide. Future experiments are planned to investigate

intermediate angles between 0 and 33 degrees, such as 15 degrees, in order to further optimize the attachment angle. This will be done along with an attachment material to help secure the transmitter on the rebar to reduce data variations and to guide more of the energy into the rebar from the larger diameter transmitter to smaller diameter rebar.

Figures 10 through 12 show each of the data plots individually, along with two theoretical exponential attenuation curves. The equation for the attenuation curve and the attenuation coefficient are determined by Equations 1 and 2, respectively.

When guided wave attenuation is considered, the attenuation coefficient (α) describes the weakening of the signal due to scattering and absorption, and can also be considered as the decay of power or intensity of a sound wave (Rose, 1999). This is defined by Equation [1].

$$A_i = A_0 e^{-\alpha(z-z_0)} \qquad \text{[Equation 1]}$$

where; A_i and A_0 are the decreased and initial amplitudes, respectively and $z\text{-}z_0$ is the distance the wave travels through the material.

In this study, when determining the attenuation coefficient of the guided wave, $z\text{-}z_0$ is the distance that the ultrasound travels in the embedded steel bar (i.e. distance between transmitter and receiver located at ends of embedded bar). When determining the attenuation of the leaked waves, $z\text{-}z_0$ is the distance between the points along the array in the z-direction or the distance between arrays in the leakage angle direction. Attenuation coefficient can be determined by Equation 2.

$$\alpha = -\frac{\log_e\left(\frac{A_i}{A_0}\right)}{(z-z_0)} \qquad \text{[Equation 2]}$$

In Figures 10-12, the two theoretical curves represent the exponential decay of the amplitude readings of the leaked waves along the length of the specimen by first assuming **a high attenuation coefficient** and **then a low attenuation coefficient**. The limits of the envelopes were previously obtained by the authors as presented in Garcia, 2016. It was found that the dimensions of the specimen tested could influence the readings. The smaller the dimensions of the specimen, more likely it would be that reflection within the concrete would be detected by the sensors which would result in larger increases of the higher amplitude readings at the starting end of the guided wave, and thus use of a higher attenuation coefficient is more appropriate. As such, the lower bound (blue dashed lines) presented here is the highest attenuation coefficient obtained from Garcia (2016), which represented the sensor arrays detecting a high volume of reflections within the concrete. The upper limit (red dashed line) is the attenuation coefficient of the leaked waves in specimens of larger dimensions, which, as expected, is the same attenuation as the guided wave itself.

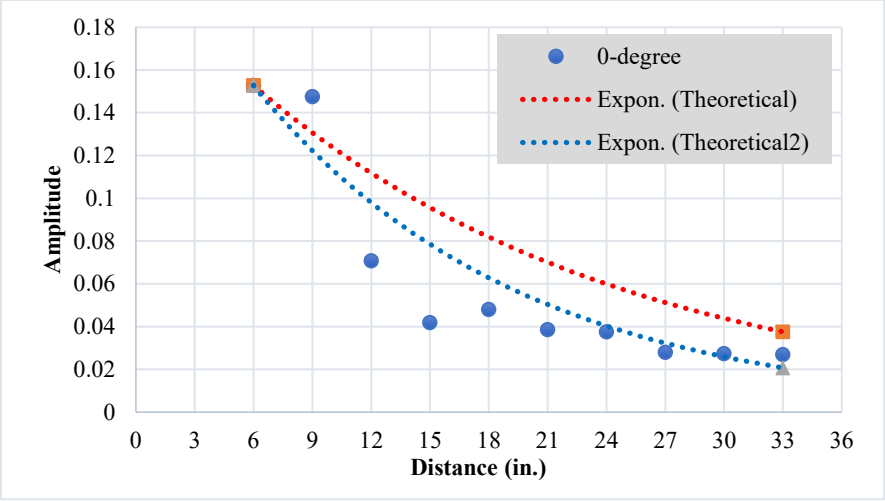

Figure 10. UGWL Data for 0-degree Specimen and Related Upper and Lower Bound Attenuation Curves

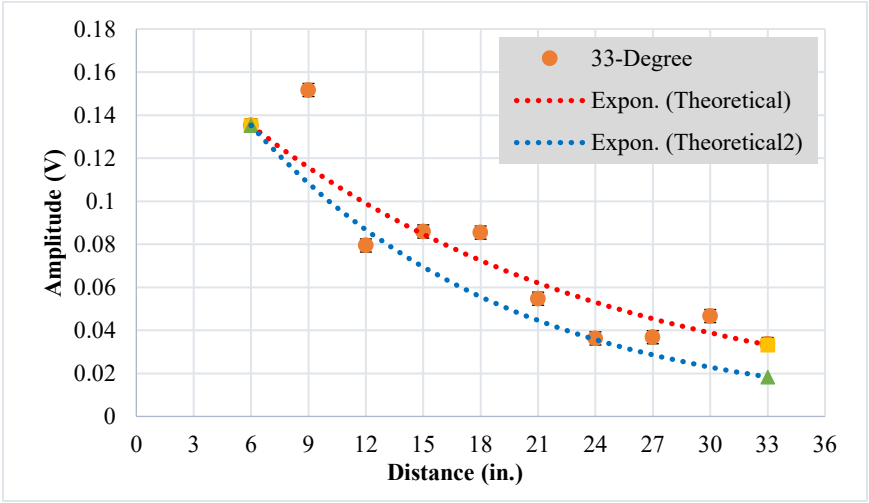

Figure 11. UGWL Data for 33-degree Specimen and Related Upper and Lower Bound Attenuation Curves

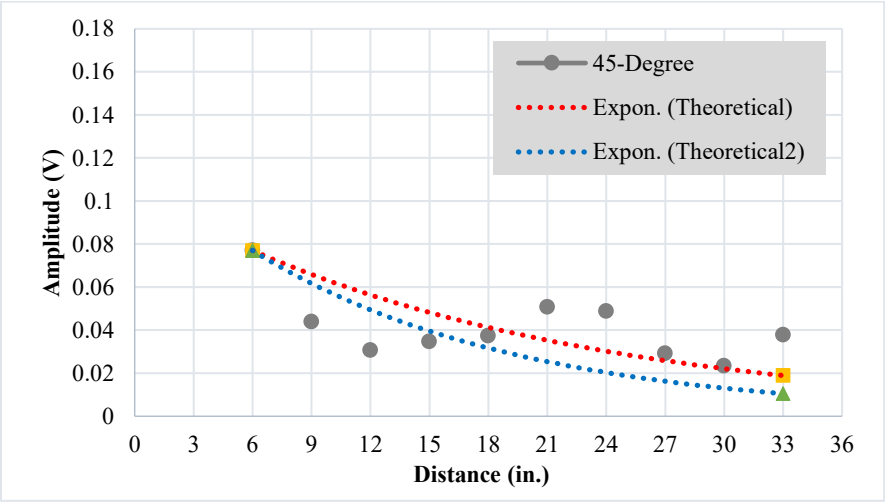

Figure 12. UGWL Data for 45-degree Specimen and Related Upper and Lower Bound Attenuation Curves

3.1.2 Results of Specimen Set 1: Effects of Couplants

Two different couplants between the sensors and the test materials (steel or concrete) are studied: (1) Ultragel II from Magnaflux; and (2) White Lithium Grease (WLG) from Lucas Oil Products. It can be seen in Figure 13 that not only is the peak amplitudes for coupling with Ultragel II slightly higher than the WLG, but also the R-squared value for curve-fit with an exponential trendline is improved. Another advantage of Ultragel II is that it can be easily wiped off the surface as opposed to White Lithium Grease. On the other hand, each data point in Figure 13 represents the average of 20 trials, and it was observed that that the standard deviation for each test location was higher with Ultragel II (noted by error bars in the plots). This is likely because it is less sticky compared to WLG and provides more room for user errors. Thus, care should be taken to ensure consistent data collection with Ultragel II. Figures 14 and 15 show the UGWL data with these two couplants on the 0-degree specimen separately as they correlate to the theoretical attenuation curves. Finally, Table 4 provides a summary of the comparison between Ultragel II and WLG considering several factors. After studying all forms of data, the difference between the coupling options is deemed to be not statistically significant and either couplant can be used in this method; however, Ultragel II appears to be slightly more efficient overall.

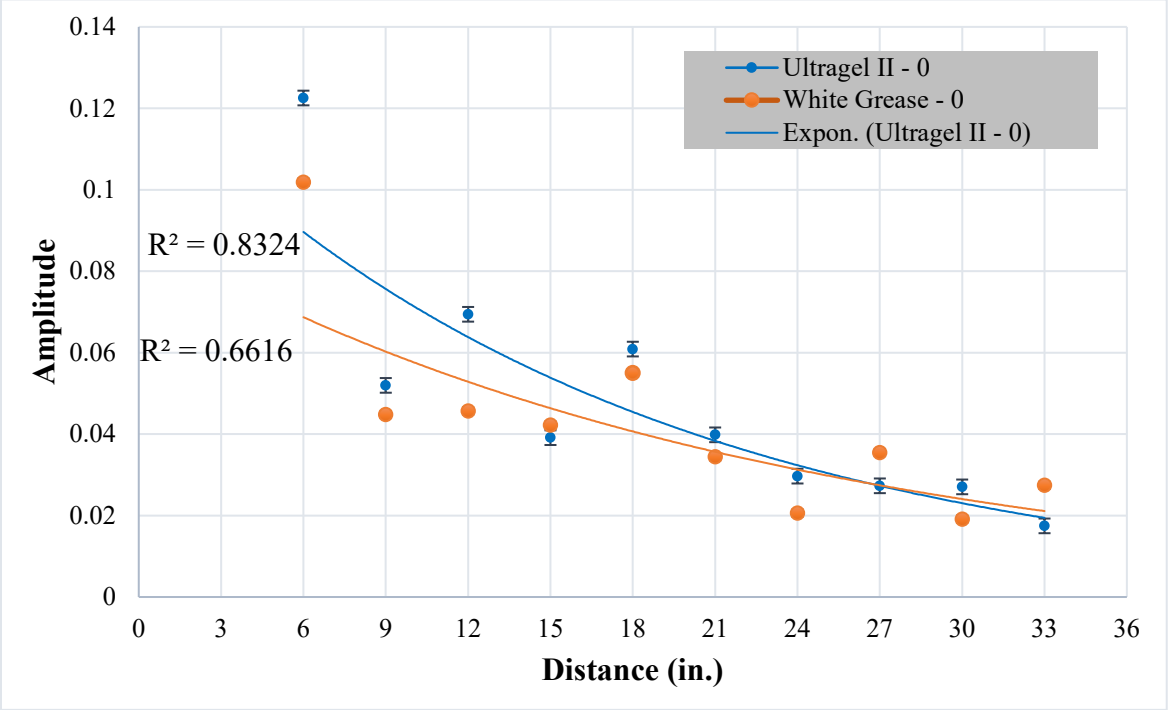

Figure 13. 0-degree Specimen: Comparison between Ultragel II and White Lithium Grease

Table 4. Comparison between Ultragel II and WLG

Comparison Category	Ultragel II	White Lithium Grease
Data consistency /repeatability	✓	✓
R-squared value	✓	
Easily wiped off from surface	✓	
Viscosity/stickiness		✓
Price		✓

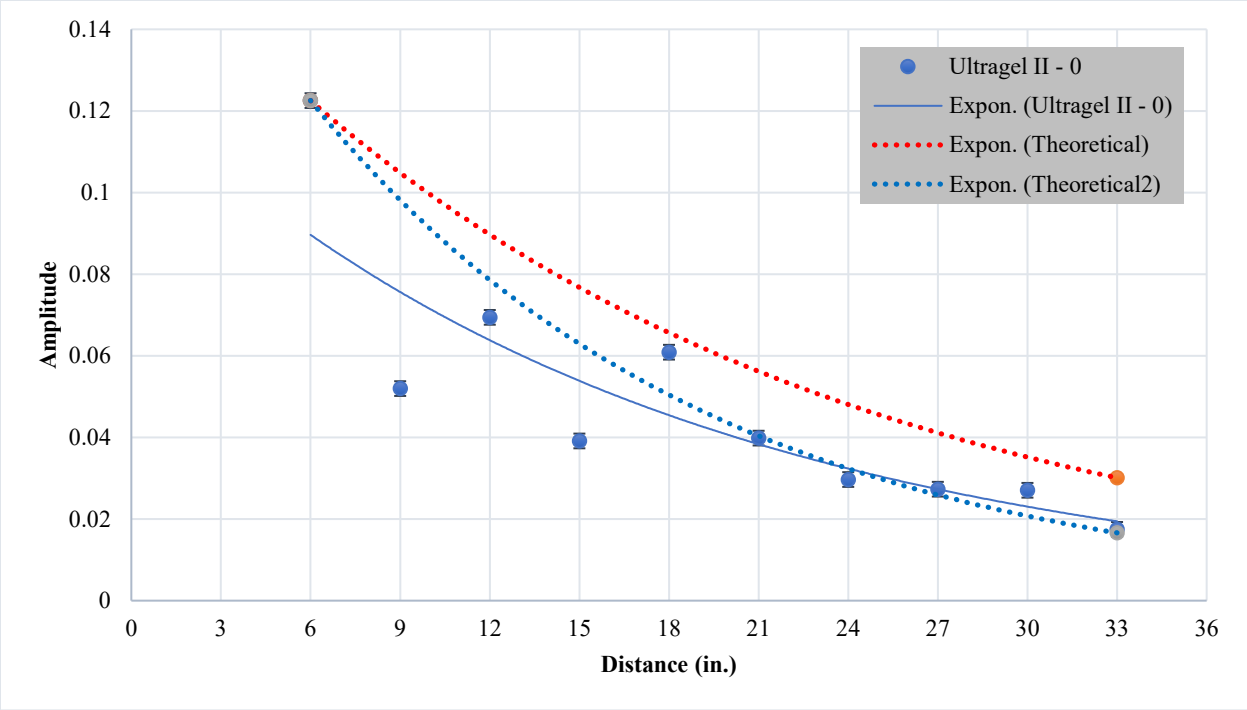

Figure 14. 0-degree Specimen: Ultragel II Results on the 0-degree Specimen

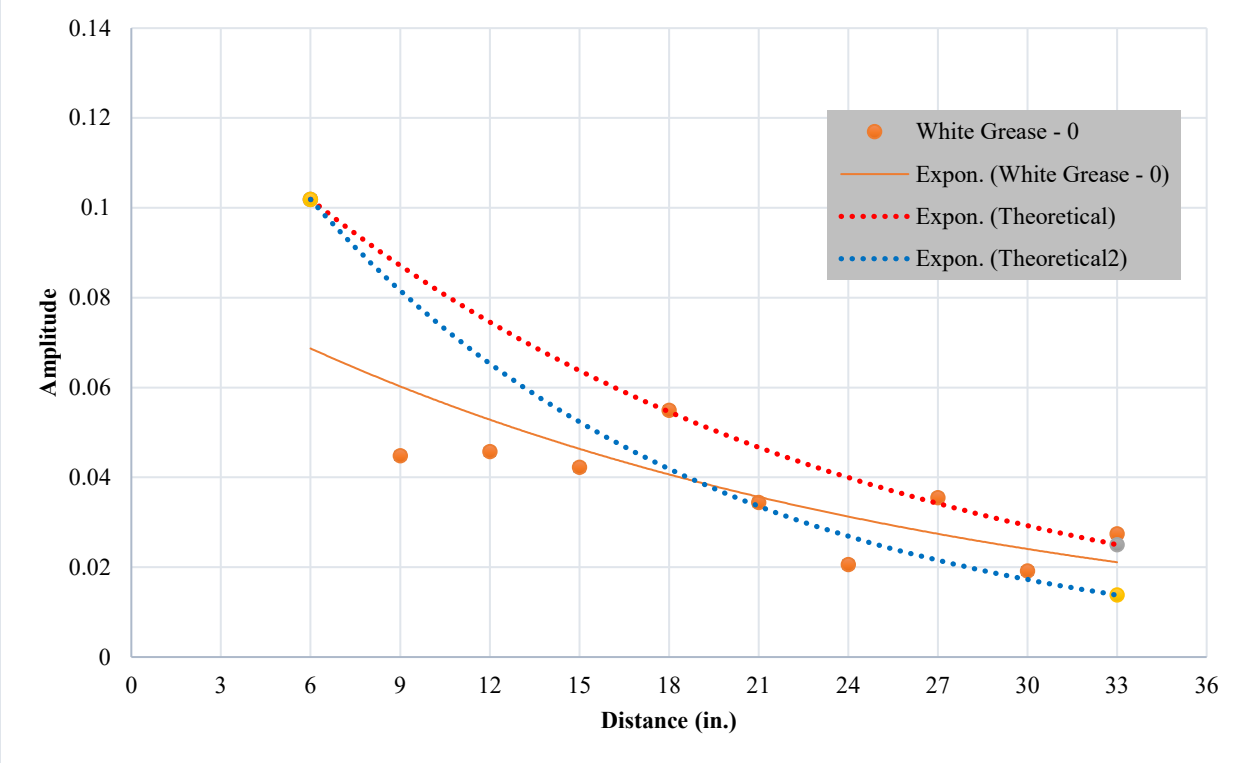

Figure 15. 0-degree Specimen: White Lithium Grease (WLG) Results on the 0-degree Specimen

3.1.3 Results of Specimen Set 1: Corrosion Monitoring via UGWL and HCP

After the investigations on different bar end angles as well as the couplants were completed, two of the specimens (0-degree and 33-degree, *henceforth referred to as Specimen A and B*) were submerged in 10% NaCl solution as shown in Figure 16. This was done in order to create a corrosive environment and monitor the changes with UGWL and HCP methods simultaneously. As the specimens were soaked in salt water environment, the UGWL and HCP data were collected every three days for first month, and then every six days to monitor the corrosion process.

Figure 16. Test specimen submerged inside 10% NaCl solution

Figures 17 through 19 present the UGWL data for Specimen A for Days 3, 6 and 9, respectively, plotted together with the baseline data taken on Day 0. Prior to the corrosion process, potential errors that may be caused by irregularities on the concrete surface were minimized by smoothing the surface with sand paper. As stated before, an increase in the measured amplitude values may indicate some corrosion activity in the locations corresponding to the sensors detecting this increase.

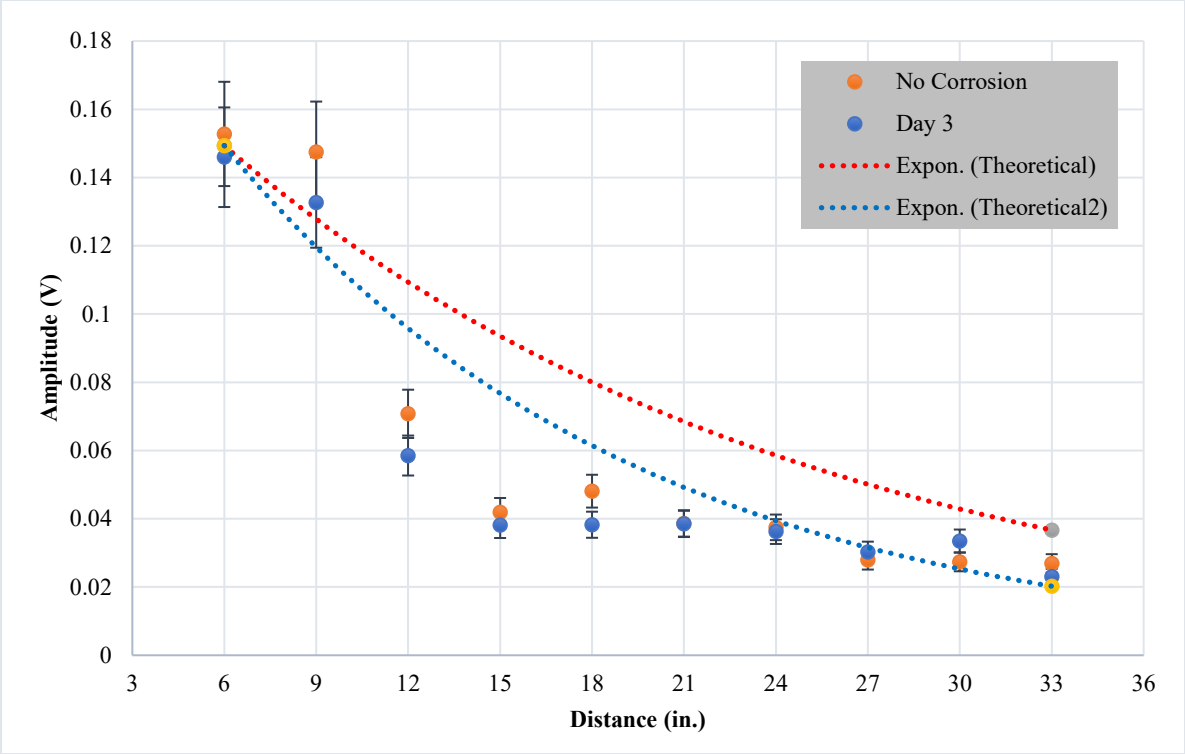

Figure 17. Specimen A- UGWL readings for Day 0 and Day 3

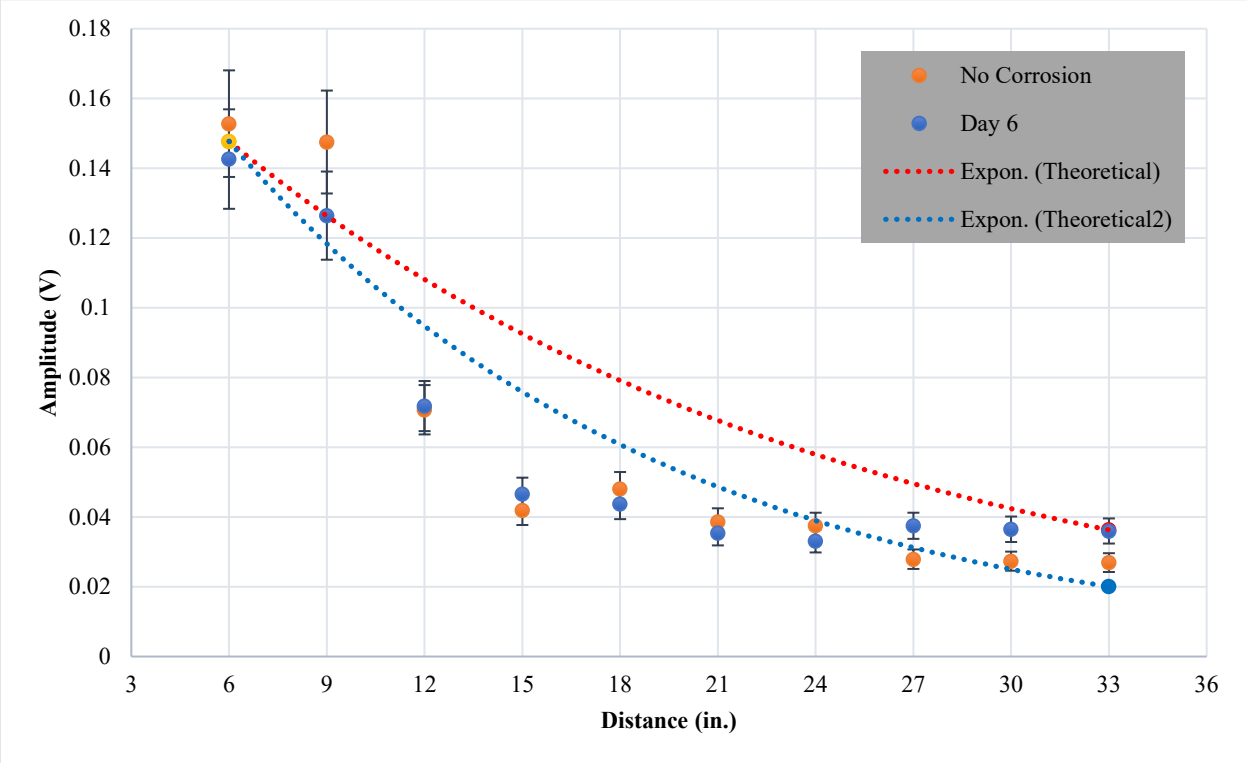

Figure 18. Specimen A- UGWL readings for Day 0 and Day 6

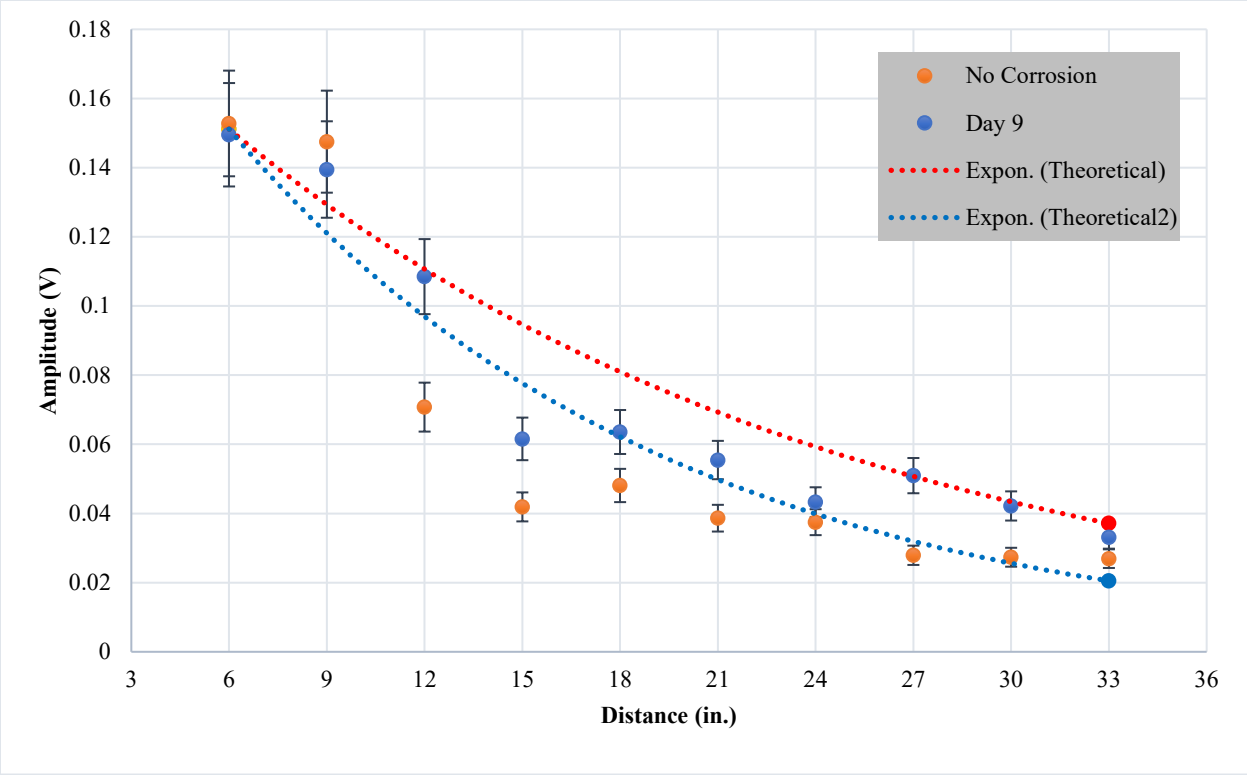

Figure 19. Specimen A- UGWL readings for Day 0 and Day 9

Figure 20 presents the combined data for Day 0, 3, 6 and 9 for this specimen. As can be seen in both Figures 19 and 20, some points, such as the sensor at 12 inches from the transmitter point, show a significant increase in amplitude of the leaked waves by Day 9.

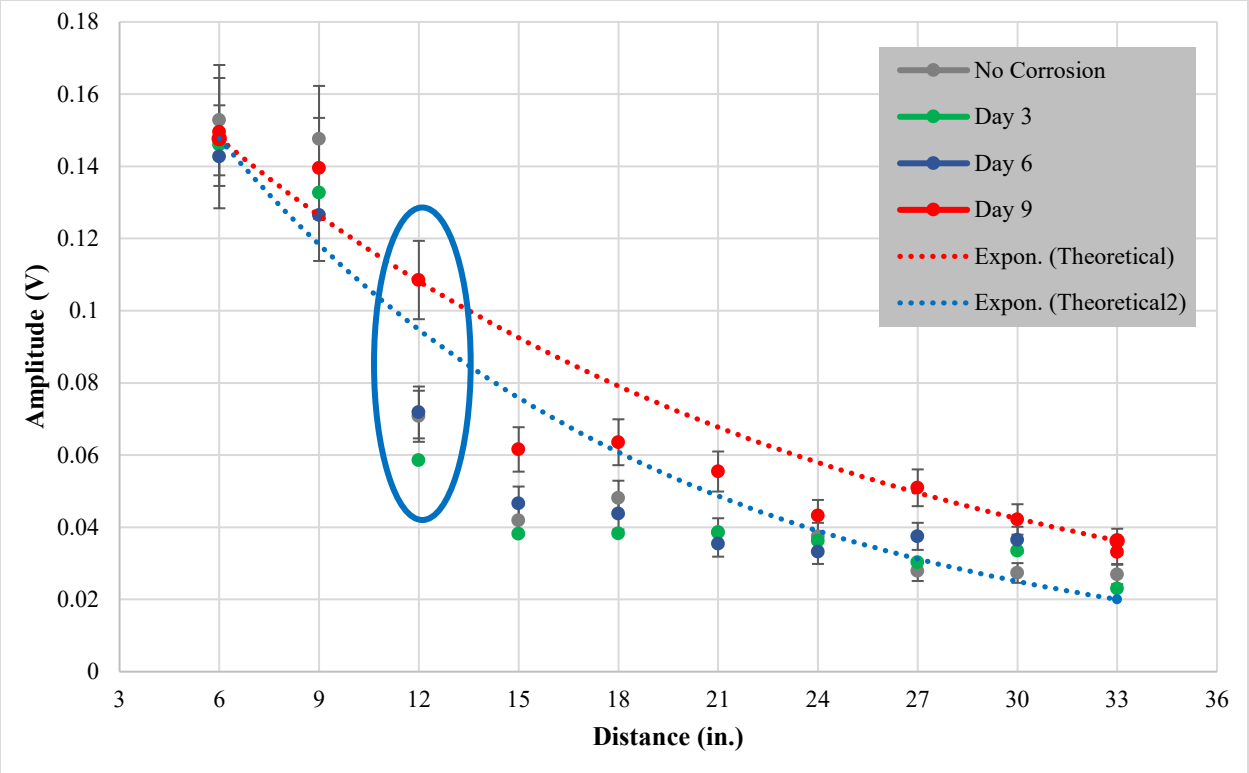

Figure 20. Specimen A- Combined plot of UGWL readings for Days 0, 3, 6 and 9

To quantify the change of amplitude in the recorded UGWL amplitudes over time Equation [3] is utilized.

$$Change\ of\ Amplitude\ (\%) = (\frac{A^i}{A^0} - 1) \times 100 \qquad \text{[Equation 3]}$$

where:
A_i - is the amplitude of 54 kHz in the frequency domain of i^{th} increment of corrosion
A_0 - is the amplitude of 54 kHz in the frequency domain before corrosion

As shown in Figure 20, a slight increase can be observed in all points measured, with the largest change at the 12-inch point. The % change in amplitude (%) between Day 0 and Day 9 for this point is computed as 53.5% from Equation [3]. Figure 21 shows data from Day 30 in comparison to Day 0. The amplitude change for the 12-inch point seems not to have increased further, and in fact a slight decrease is noted, potentially indicating a change in the nature of the deterioration at this locale. The sensor at 15 inches from the transmitter, on the other hand, shows the largest increase in amplitude on Day 30. The percent change between Day 0 and Day 30 for Point 15 is calculated as 95%, which is quite significant.

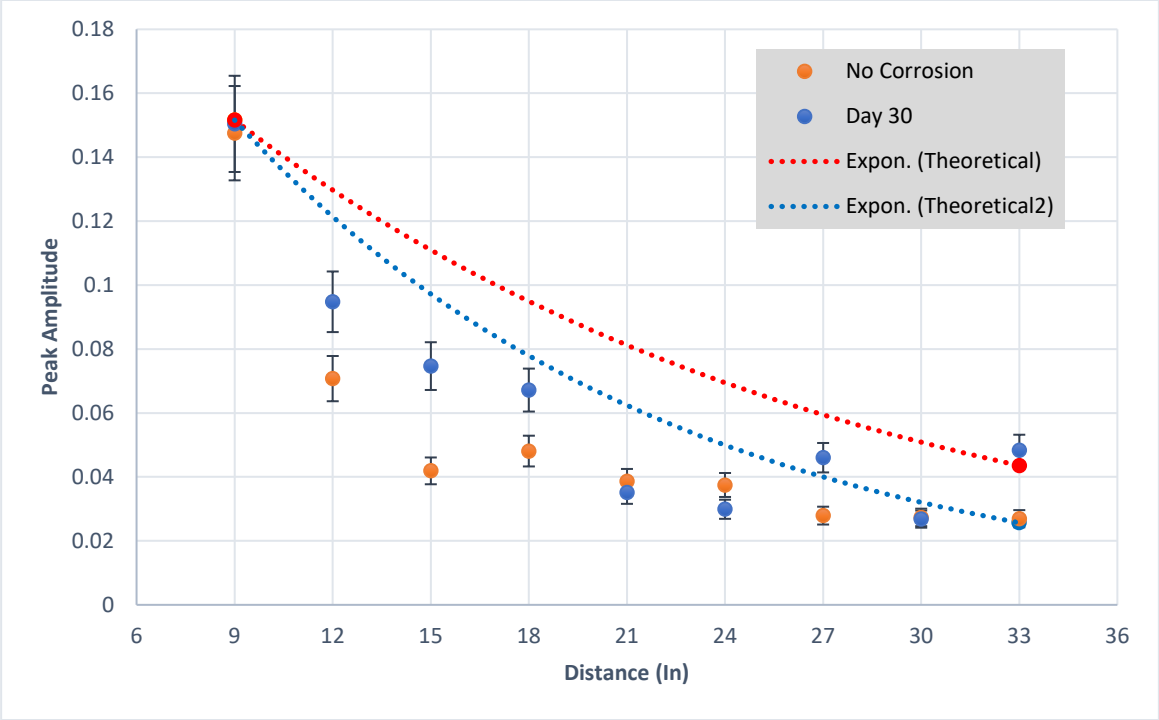

Figure 21. Specimen A-UGWL readings for Day 0 and Day 30

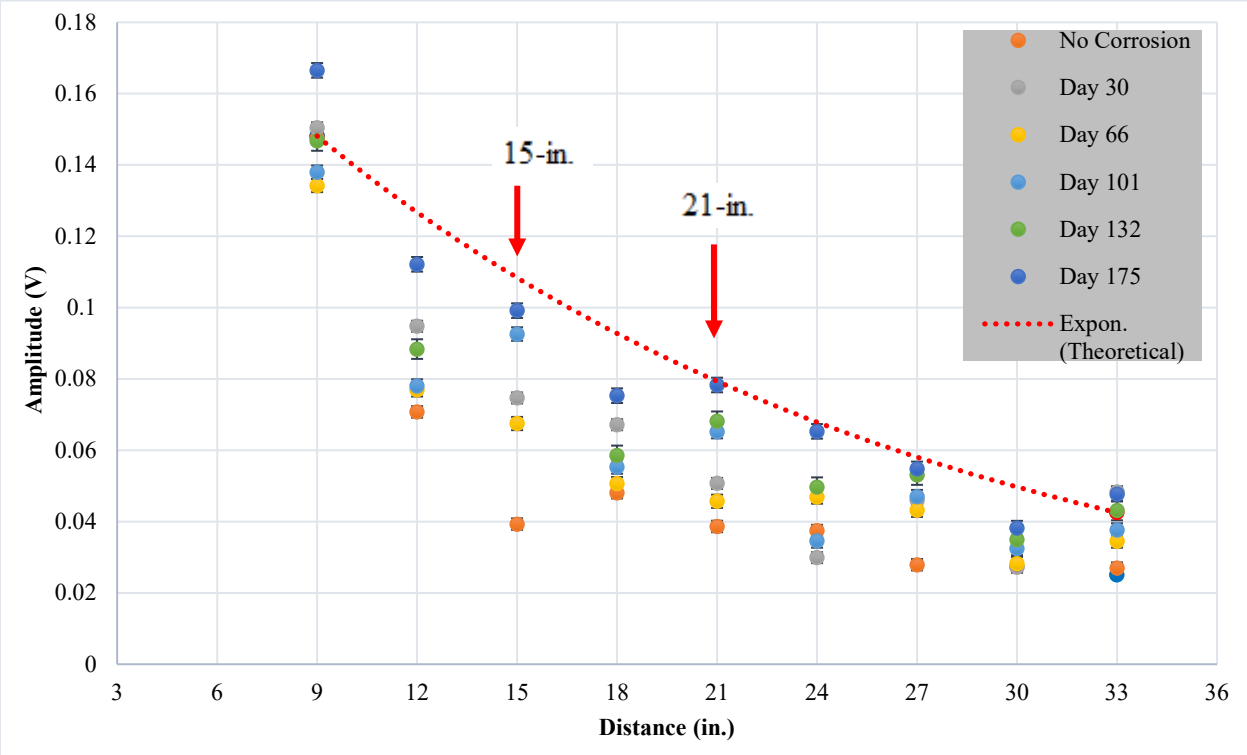

Figure 22. Specimen A- UGWL readings combined plot for 0-175 days

Figure 22 presents select days of data from Day 0 up to 175 days for the full array of sensors. It can be seen that the most significant changes over the entire period of monitoring are observed at points 15 inches and 21 inches from the transmitter end.

Figure 23 further illustrates the change in amplitude for these two points over the entire duration of the experiment, *i.e.* 175 days, for this specimen. Given the specimen is continuously soaked in NaCl water during this period, without any other interventions or change in circumstances, the changes in the UGWL amplitude are directly attributed to corrosion progression.

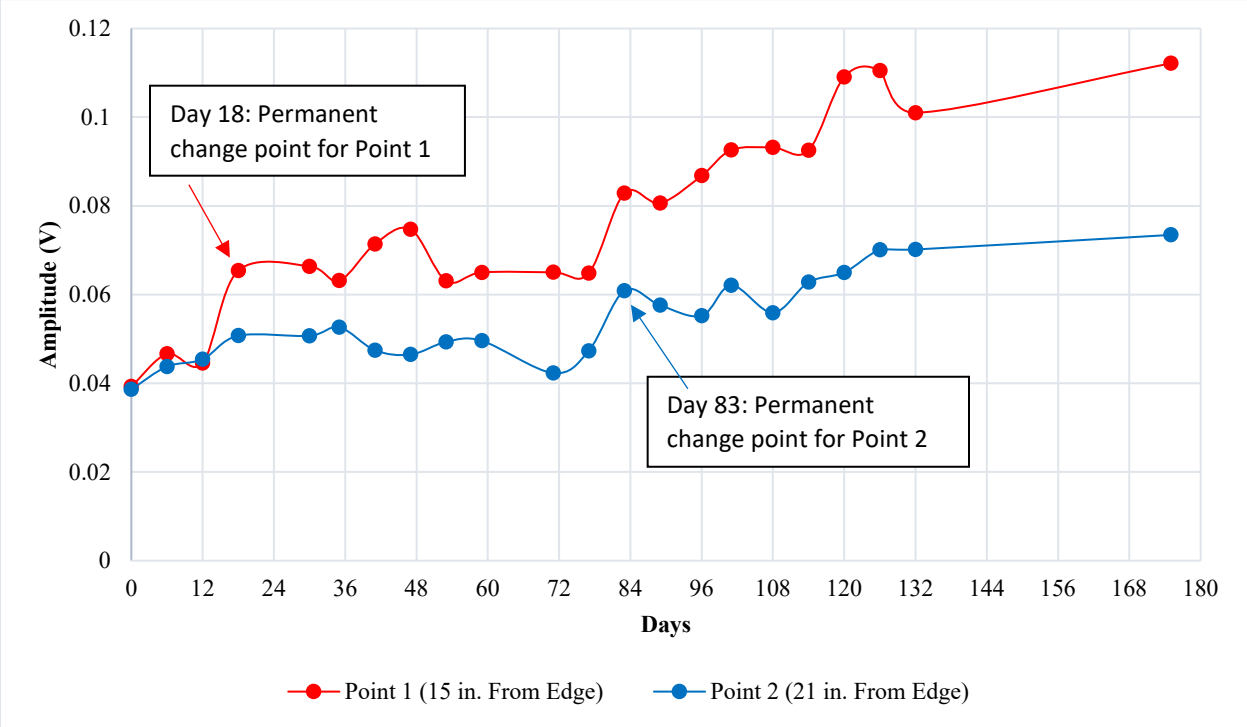

Figure 23. Specimen A: UGWL amplitude change for two sensor points over 175 days

As can be seen in Figure 23, the UGWL amplitudes do not increase linearly and some data fluctuation occurs. This fluctuation is attributed to an expected level of testing/user errors (such as sensor location being slightly of center compared to the previous test, amount of couplant used not being exact, etc.) as well as the effects of ambient noise. However, when the change in the condition is significant enough (*i.e*. when the corrosion product build up is significant), there is a significant (or "permanent") change in the amplitudes recorded. Table 5 quantifies the change in amplitude for these two points over the entire duration of the experiment. The 175th day percent change in the amplitudes for the 15-inch point is approximately 154%, while for the 21-inch point it is 105%. When the general trend is studied, regardless of the day-to-day fluctuations, a permanent change in amplitude happens after a 50% change is established. This happens at Day 18 for Point 1 (15 inches from the edge) and Day 83 for Point 2 (21 inches from the edge). As such, this change in amplitude (50%) is suggested as a potential trigger point for "significant change in condition of the reinforced concrete slab". Anything below 50% can be considered "uncertain" or "mild deterioration potential" similar to the HCP considerations. The second specimen is studied below, to further this consideration. Later, when correlated to chloride levels, the percent changes in amplitude will be further quantified in terms of the level of the corrosion progression.

Table 5. Change of amplitude for various points for Specimen A

UGWL Sensor Locations from Transmitter End	Day 0	Day 9		Day 30		Day 101		Day 175	
	Amp. (v)	Amp. (v)	% change vs. Day 0	Amp. (v)	% change vs. Day 0	Amp. (v)	% change vs. Day 0	Amp. (v)	% change vs. Day 0
15-in.	0.039	0.061	**56**	0.074	**90**	0.092	**136**	0.099	**154**
21-in.	0.038	0.055	**45**	0.051	**34**	0.065	**71**	0.078	**105**

Figure 24 shows data for Day 175 in comparison to Day 0 for Specimen B. It can be seen that there is an overall increase of amplitudes between Day 0 and Day 132, in the range of 40 and 154 percent for all measurement points.

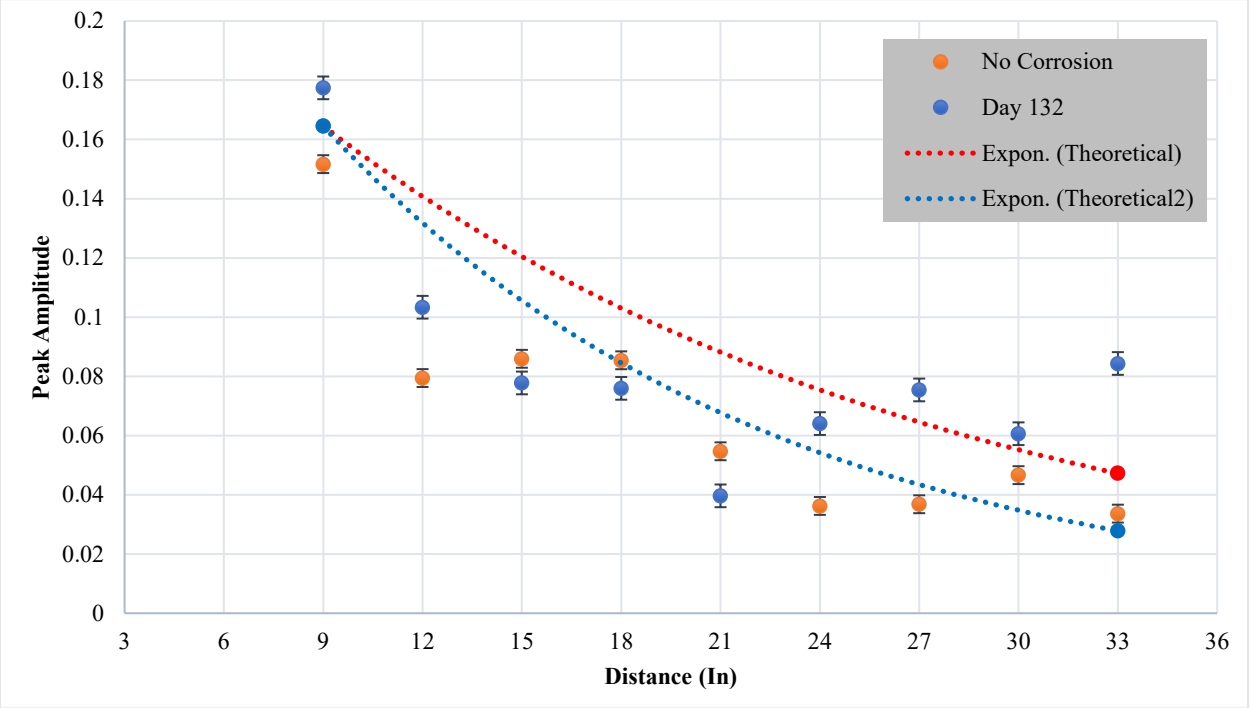

Figure 24. Specimen B- UGWL readings for Day 0 and Day 132

Figure 25 further illustrates the progression of UGWL amplitudes over time for Specimen B for all measurement points; while Figure 26 provides a daily plot showing the variation of amplitudes for two specific points. The two points selected for further investigation are 9 inches and 27 inches away from the transmitter end, because these areas demonstrated the most significant changes in UGWL amplitudes (17 and 151 percent over the 132 days, respectively). To establish some data verification, after monitoring Specimen B for 132 days using the UGWL method, an autopsy was carried out as shown in Figure 27. Some early/mild corrosion build-up can be seen on the rebar that was embedded in this specimen, which confirms the relatively low change in amplitudes. The generally lower amplitudes and the relatively weak data trend compared to Specimen A are due to the fact that the transmitter is

attached to the 33-degree cut angle in this case. This experiment confirms that even relatively small changes (such as 17%) in amplitude can indicate the start of a corrosion process.

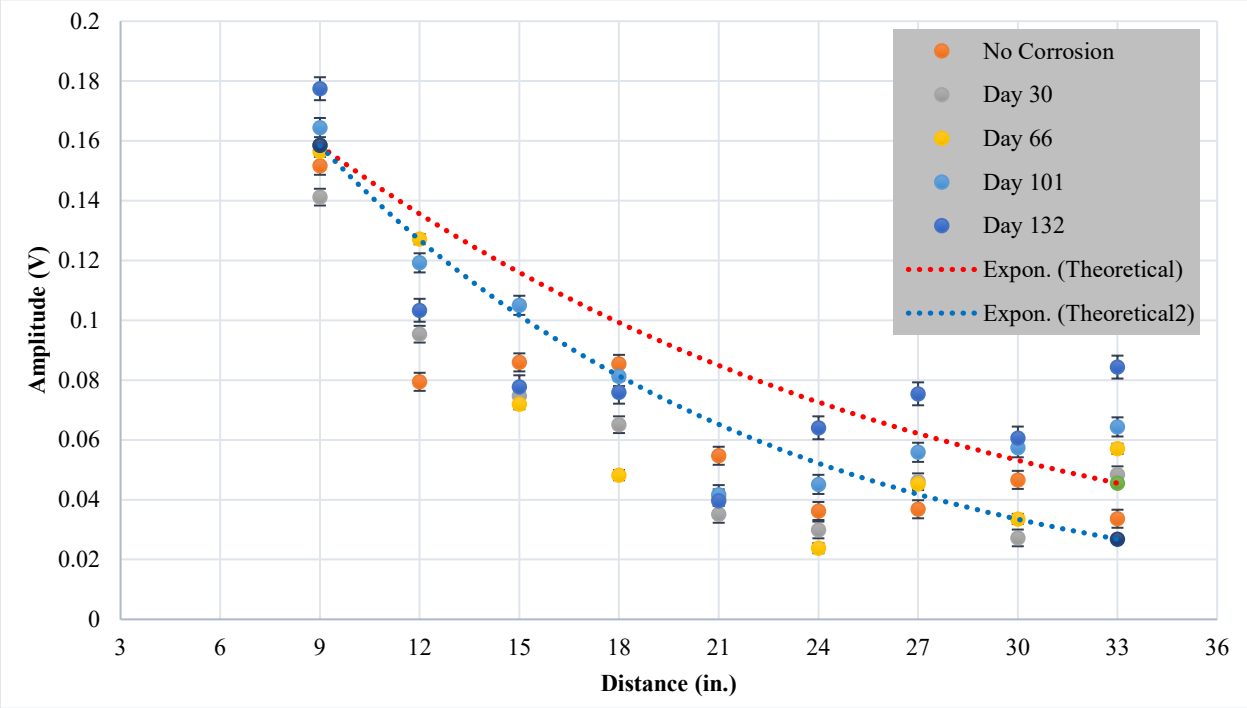

Figure 25. Specimen B- UGWL readings for select days between Day 0 and Day 132

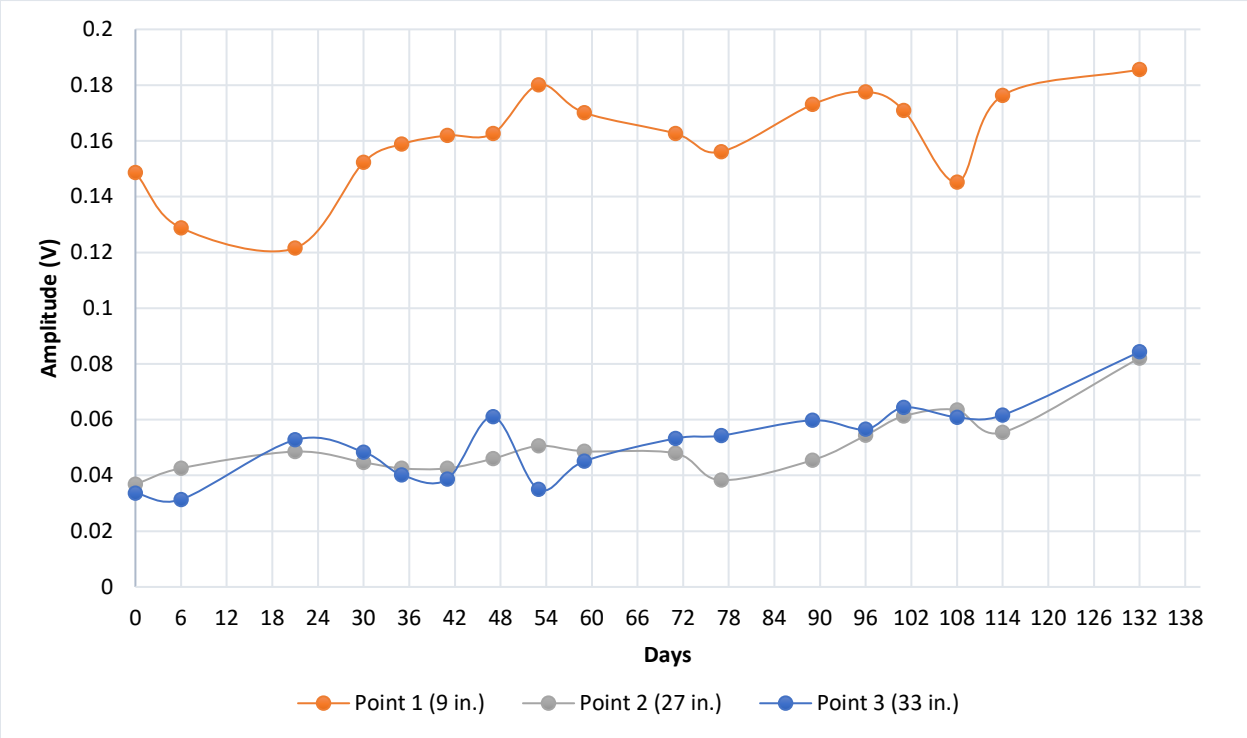

Figure 26. Specimen B- Progression of the UGWL readings from two points over time

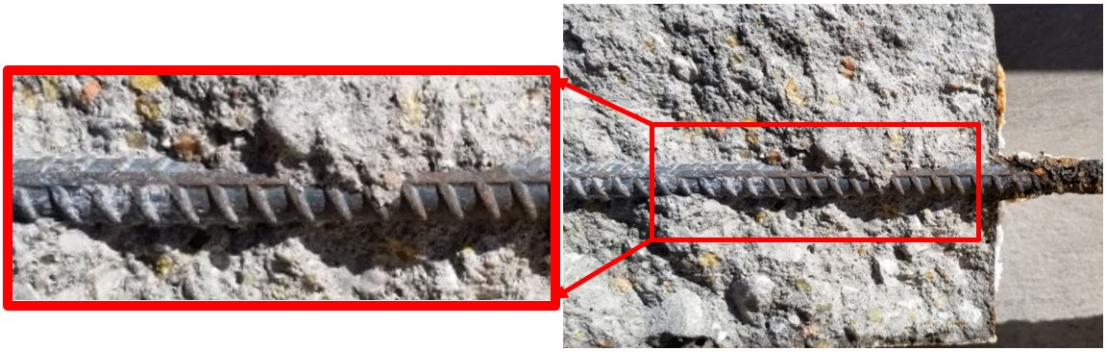

Figure 27. Specimen B- Day 132 condition verification: Very mild corrosion build-up on the rebar

Half-Cell Potential (HCP) Measurements

HCP measurements were collected on the same two specimens using the iCOR device every 6 days in conjunction with ultrasonic testing. Five test locations were marked along the rebar on the concrete surface as shown in Figure 8 (b). The HCP measurements are recorded in terms of volts, and ASTM C876 provides a correlation between the probability of corrosion activity and the voltage readings as shown in Table 1. Figures 28 and 29 show the HCP data from the two specimens, and the dotted lines demonstrate the aforementioned probability thresholds specified by ASTM C876.

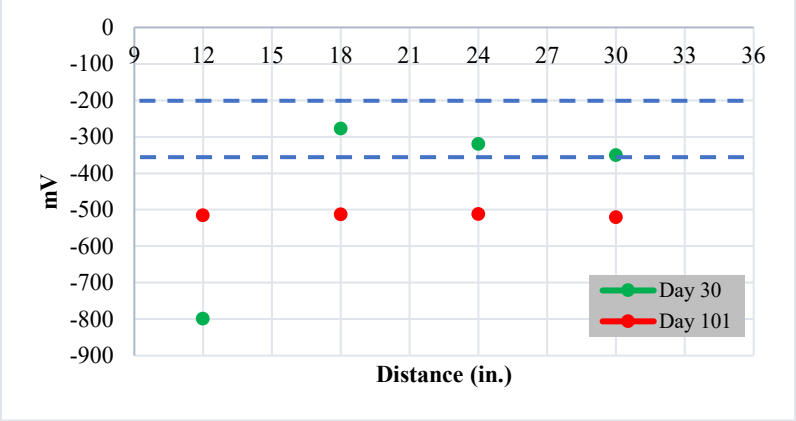

Figure 28. HCP measurements for Specimen A

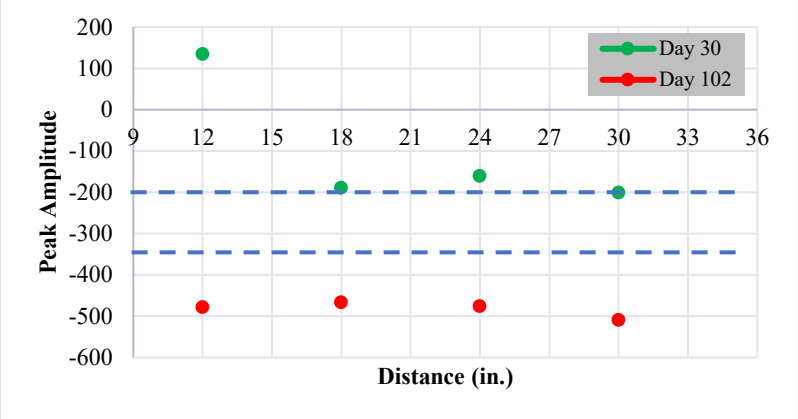

Figure 29. HCP measurements for Specimen B

From Figure 28 showing the results for Specimen A, it can be seen that majority of the HCP data for Day 30 are in the 'uncertain' region according to ASTM C876, meaning that probability of corrosion activity can be anywhere between 10% and 90%. Only the 12-inch point on this specimen showed higher probability of activity per HCP data. In general, it can be stated that, on this specimen the HCP data started showing an increased probability of corrosion by Day 30. In contrast, UGWL data, showed some increase in the amplitudes as early as Day 9, and by Day 18, there were statistically significant changes in amplitude for some of the points.

For Specimen B, HCP data is shown in Figure 29. All of the points measured on Day 30 are in the lowest probability (less than 10%) range for corrosion activity according to HCP data, and the first significant change noted according was on Day 35. While some corrosion activity was detected by the UGWL method earlier than the HCP method on Specimen B, the results of the two methods are in good alignment in that there is less potential/evidence of corrosion activity for this specimen in general. This is also in alignment with the observations from the autopsy (Figure 27). The earliest significant variations observed in the data from both techniques are indicated in Table 6.

Table 6. Earliest significant change in data

Specimens	Earliest date of significant change in data	
	UGWL	HCP
Specimen A	Day 9	Day 30
Specimen B	Day 30	Day 35

In addition to the potential of UGWL to detect corrosion progression sooner, it also has the following advantages over HCP as determined by our previous work (Garcia *et al.*, 2017 and 2019; Erdogmus *et al.,* 2020):

- UGWL can be used on epoxy-coated bars, but HCP cannot.
- UGWL can detect other flaws along with corrosion, but HCP cannot.
- UGWL transmitter can be embedded during construction, therefore not requiring coring later; while typical HCP measurements involve coring, attaching to a rebar, and taking instantaneous readings. This may establish UGWL as a quicker and a truly-nondestructive method, reducing lane closure times and coring damage.

3.1.4 Results of Specimen Set 1: Chloride Content Analysis

Chloride content analysis was conducted on Specimen A after 175 days of soaking in NaCl solution and data collection, in order to establish a quantitative correlation between the chloride content and UGWL measurements. Corrosion is initiated once chloride content reaches a certain level called critical chloride content or chloride threshold level (CTL). Since UGWL amplitudes showed the highest increase in magnitude for two specific points on this specimen (Points 15 inches and 21 inches from the transmitter), cores were extracted from these two locations as shown in Figure 30. An additional core was taken at the 30-inch location for comparison purposes. The extracted cores were then broken into smaller pieces to be converted to a pulverized form that is necessary for chloride analysis as shown in Figure 31.

Figure 30. Extracted cores from the concrete specimen

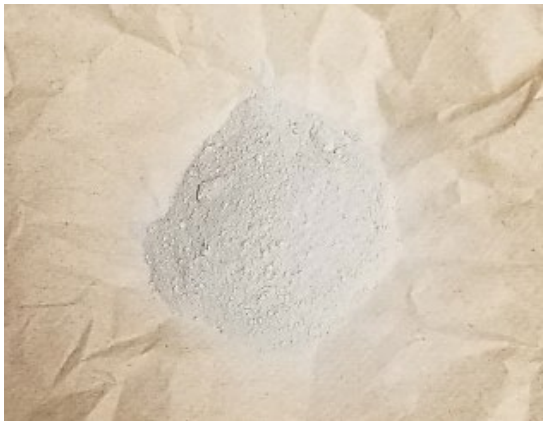

Figure 31. Concrete sample in pulverized form

The pulverized concrete samples were then sieved using a No. 20 sieve (850 µm) as recommended by ASTM C1152 (ASTM, 2012), which provides guidance on the acid-soluble test to determine chloride content in concrete. The samples were then mixed properly to make them homogenized. In order to perform the analysis, 2 gm of each sample was mixed with 5 mL of nitric acid and Methyl Orange Indicator inside beakers. After the color of the samples turned pink, the samples were placed on a heat plate until they started boiling. The samples were then filtered using filter paper inside flasks to remove any residuals or particulate matters. The final solutions were prepared inside volumetric flasks with 250 mL of purified water. Ion Chromatography was performed using Eco IC Chromatography System from Metrohm shown in Figure 32. Each sample was tested using this device to determine the concentrations for different ionic species such as fluoride, chloride, nitrate, nitrite, and sulfate. This test ultimately provides the total chloride level present in the concrete samples per weight of concrete. Two iterations were performed to get more reliable results. In addition, purified water was also tested in order to verify the validity of the results, and hypothetically, purified water should indicate a very low level of chloride concentration.

Figure 32. Eco IC Chromatography System from Metrohm

The results for the first and second iteration of chloride content analysis are given in Tables 7 and 8, respectively; and the average of these iterations per sample are provided in Table 9.

Table 7. Percentage of chloride content per weight of concrete (1st iteration)

Sample	Mass (g)	Volume (L)	Solution (ppm)	% Cl per Concrete weight
Purified Water	-	-	0.128	-
15-inch	2.1008	0.2500	70.62	0.84%
21-inch	2.1037	0.2500	47.486	0.56%
30-inch	1.9880	0.2500	15.181	0.19%

Table 8. Percentage of chloride content per weight of concrete (2nd iteration)

Sample	Mass (g)	Volume (L)	Solution (ppm)	% Cl per Concrete Weight
Purified Water	-	-	Not Detected	-
15-inch	2.0425	0.2500	68.745	0.84%
21-inch	1.9692	0.2500	42.667	0.54%
30-inch	2.0100	0.2500	14.209	0.18%

Table 9. Percentage of chloride content by weight of concrete (Average of two iterations)

Sample	Average % Cl per Concrete Weight
15-inch	0.84%
21-inch	0.55%
31-inch	0.185%

All of the results (Tables 7-9) exceed the CTL specified by Technology in Practice (TIP), which ranges between 0.05 to 0.1% by weight of concrete. As such, it can be concluded that chloride content in this specimen has exceeded the chloride threshold values and corrosion activity has definitely started by Day 175.

Table 10 provides the quantitative correlation between the percent change in the amplitudes from UGWL data collected for Points 15-inch and 21-inch in Specimen A at Day 175 (right before CTL check), as well as the percent chloride content in the concrete specimen. 15-inch Point represents the highest percentage change in UGWL amplitudes, as well as a much higher chloride content concentration at this location compared to 30-inch point, for instance. **In general, almost a directly proportional relationship is observed between the UGWL readings and chloride content.** The correlation is reiterated in Figure 33. **Further, there is strong correlation between the HCP data, CTL levels, and UGWL readings (Table 10).**

Table 10. Correlation between CTL and UGWL data

Measurement Location	UGWL Data			HCP Data		
	Day 0 (Amplitude)	Day 175 (Amplitude)	Percentage Change in UGWL reading (%)	Day 175 Reading (mV)	Day 175 Probability of Corrosion Activity	Average %Cl per Concrete Weight
15-inch	0.039	0.099	154 %	-624	>90%	0.84%
21-inch	0.038	0.078	105 %	-595	>90%	0.55%
30-inch	0.027	0.038	40 %	-574	>90%	0.185%

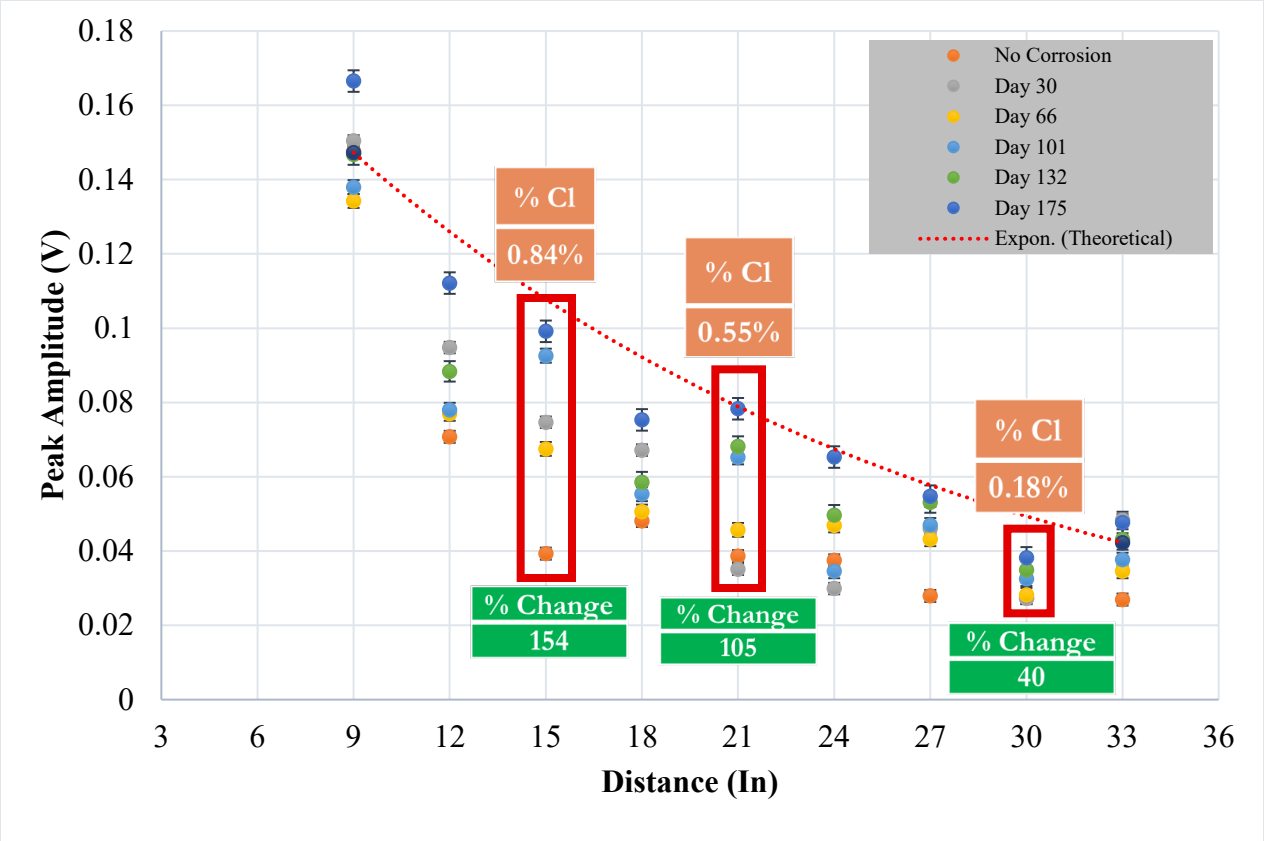

Figure 33. Correlation between UGWL data and chloride content

3.2 Specimen Set 2

The aim of this set of experiments was to explore different sensor-to-rebar attachment materials for improved coupling. For this purpose, laboratory experiments were conducted using a 16 mm (No. 5) rebar. Energy was transmitted into the rebar using five different methods as listed below and shown in Figure 34:

1) The transmitter was coupled directly to the end of the rebar;
2) A 5.1 cm (2 in.) section of the rebar was ground flat and the sensor was attached onto the rebar using a typical grease couplant;
3) A lead solder pad was created, where a sheet metal form was placed over the bar; sand was placed around the form as a seal to prevent solder leakage, and lead solder was melted onto the pad with a torch. The pad was filed flat after cooling;
4) A seat for the transmitter was created using steel-filled JB Weld epoxy, poured into a form around the bar; and
5) A seat for the transmitter was created using Hydrocal gypsum cement, poured into a form around the bar.

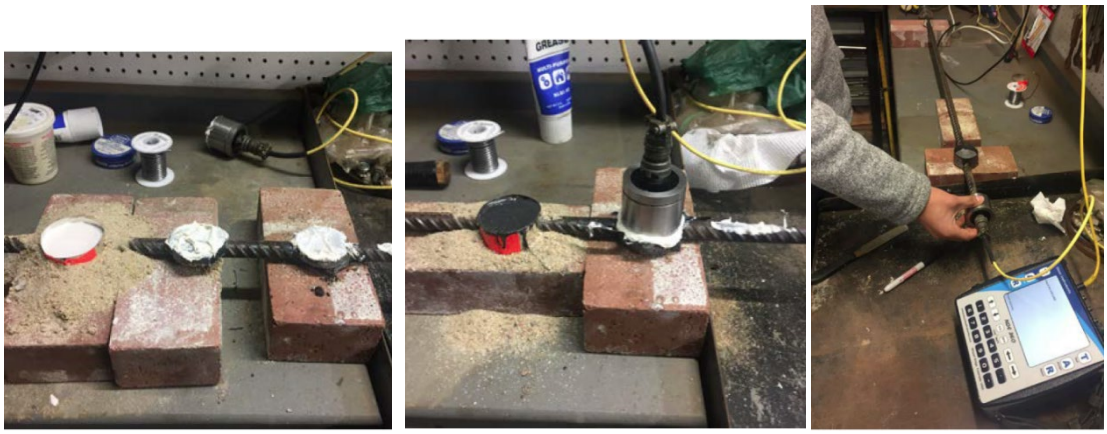

(a) (b) (c)

Figure 34. Attachment options: (a) Direct energy transmission; (b) Transducer coupled to solder pad and epoxy pad curing in sheet metal form; and (c) Solder and epoxy pads fully cured. Gypsum cement poured into sheet metal form

Signals were recorded using an Olson Instruments NDE 360 ultrasonic system. Two-inch ultrasonic transducers operating at a center frequency of 50 kHz were used, similar to the other experiments. The receiving transducer was attached to the rebar end using hot-melt glue. The transmitter was coupled using white lithium grease at each transmitter station. For each trial, the recorded waveform energy was measured as a percentage of the full scale, normalized against the system's peak voltage input. This technique permitted simple comparison of waveforms recorded using each coupling procedure.

The experimental results (Table 11) showed that the maximum energy transfer was achieved when the transmitter was coupled directly to the end of the rebar, which represents the original lab setup and aligns with the optimal wave propagation expected with wave guides. The second highest amplitude measurements were obtained using the Hydrocal gypsum cement, despite a perpendicular attachment to the rebar. This material also has a relatively fast curing time of approximately 20 minutes; thus it will not cause significant delays while field testing.

Table 11. Attachment alternatives tested

Transmitter Position	Path Length (m)	% Full Scale
End of bar	1	43
Flat ground area	0.94	4.6
Lead solder pad	0.86	18
Steel-filled JB Weld epoxy	0.746	23
Hydrocal Gypsum	0.63	32

In conclusion, Hydrocal gypsum is recommended for attaching the transmitter to rebar and embedment in concrete for field applications. It should be noted, however, that gypsum needs to be protected against environmental elements using a water-proof wrap or similar.

3.3 Specimen Set 3

To further investigate the corrosion progression in reinforced concrete slabs, 8 specimens measuring 36 x 18 x 5 inch were cast, each with a number 4 rebar embedded at mid-depth. Figure 35 shows the

specimens that were cast in the Omaha/PKI Structures Laboratory of the University of Nebraska-Lincoln. 47BD mix was used to cast these specimens, similar to previous specimens. Out of these specimens, 6 slabs were cast for corrosion-to-delamination monitoring, and 2 specimens for further assessment of sensor-to-rebar attachment embedded in the slab.

The corrosion specimens consisted of two parts: (1) 3 specimens cast with clean bars; and (2) 3 specimens cast with corroded bars that were exposed to 10 NaCl concentration. One end of the rebars embedded in the corrosion specimens were cut at a 15-degree angle with respect to vertical axis, and left as it is (i.e. 0 degrees) on the other end, as shown in Figure 36.

Figure 35. Specimens Set 3

Figure 36. Bar end angles for corrosion specimens in Specimen Set 3

The two specimens used for further testing of the Hydrocal attachment and embedment were designed as follows: One of the two specimens for testing the embedded attachment was cast using a No.4 longitudinal rebar, and the other one was cast using one longitudinal bar and four transverse bars. One sensor was embedded in each specimen using a Hydrocal Gypsum cement angled at 15 degrees as shown in Figure 37. A cable was attached to the sensor on one end, and the other end was left outside of the formwork, so that the transmitter can be attached while performing UGWL measurements at later stages in the experimental work. These sensors and the gypsum seats were then wrapped using duct tape to avoid contact with water and concrete, as shown in Figure 37(b).

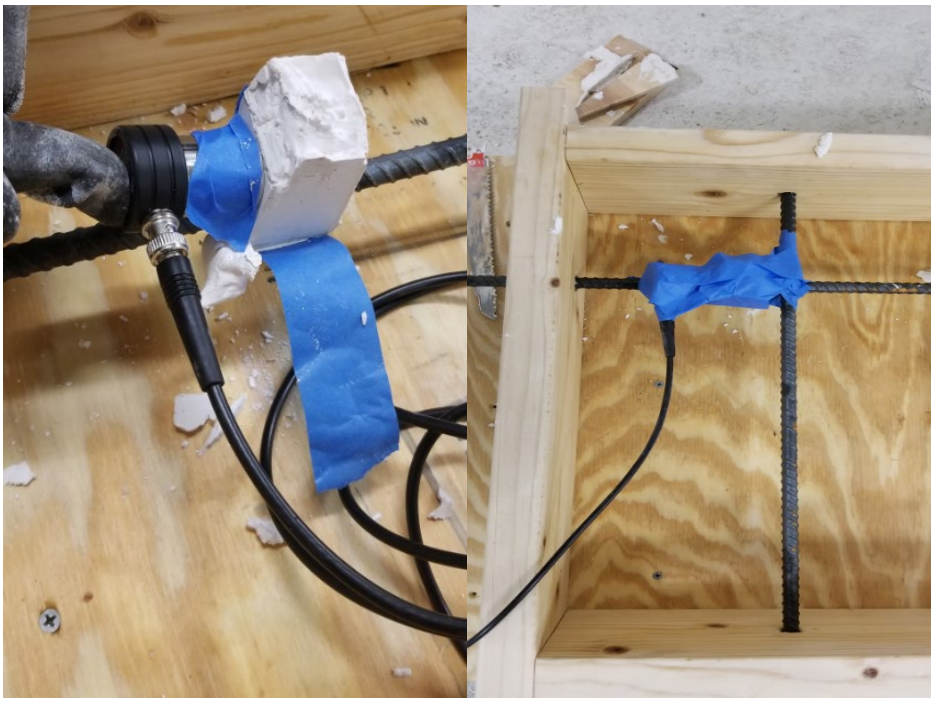

(a) (b)

Figure 37. Sensor-to-rebar attachment: (a) sensor attached to the rebar using gypsum; (b) the sensor shown in (a) is wrapped using duct tape

While these specimens were cast in January with the intention to include some of the results in this project's report, due to the COVID-19 pandemic and the following shutting down of the university buildings and laboratories, the experimental program was halted after casting. It is the PI's intension to still pursue these experiments and include the findings in future technology transfer documents such as the final report of NDOT Project M113 and another journal publication.

4. Field Implementation

A field implementation study was performed on the Dwight East Bridge near Valparaiso, Nebraska; structure number S066 06060 (*henceforth referred to as the "Valparaiso Bridge"*). Figure 38 shows the location of the embedded sensor with respect to the measurement box placed on the shoulder. A transmitter was attached to a number 4 transverse, epoxy-coated rebar located on the west side of the bridge deck while it is under construction, as shown in Figure 39 (a). Hydrocal gypsum cement was used to permanently attach the transmitter to the rebar at that location. The attachment was then wrapped

with a water-proof duct tape. A BNC RG58 coaxial cable was connected to the sensor at one end, and the other end of the cable was enclosed inside a water-proof box to stay outside on the side of the bridge as shown in Figure 39 (b). After the arrangement was made the concrete was cast. More photos from installation can be found in the Appendix.

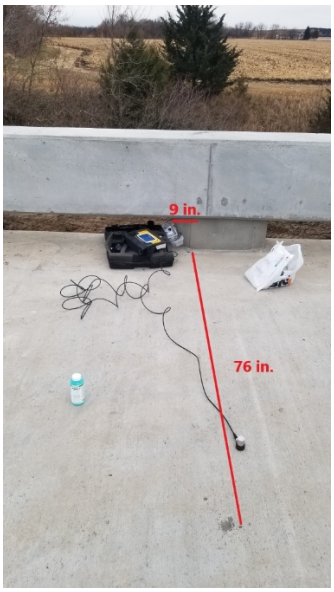

Figure 38. Location of the sensor with respect to the reference point (location of the measurement box)

Figure 39. Valparaiso Bridge Instrumentation: (a) gypsum seat attachment of the ultrasonic transmitter wrapped in duct tape; (b) Sensor cable is protected inside a protective duct and ran to the side of the bridge

After the concrete was cured and the bridge was ready for monitoring, the first set of data (baseline) was collected using PULSONIC Ultrasonic Pulse Analyzer 58-E4900 (shown in Figure 5). The transmitter is located approximately 77 inches from the edge of the bridge, which is the first point for data collection along the rebar. The testing was carried out along the rebar on the bridge in the transverse direction,

covering a full lane and part of the other lane, resulting in a coverage length of 14 feet. This distance was established previously in NDOT project M066, where a pilot test was conducted on a bridge near Emerald City.

Ten readings were collected for each test location for first few locations, where the distance between the sensors is less. This is because the ultrasonic measurements are more sensitive for a shorter distance between the transmitter and the sensor are shorter due to the reflections of shear and longitudinal waves. Thus, more data is collected for improved repeatability for the earlier locations. For other test locations, *i.e.* as the distance between the sensors increases, five readings were collected for each test spot. Figure 40 shows combined plot of the measurements collected on different dates along with the baseline data using UGWL method. The wave energy attenuated exponentially, such that as the distance between the transmitter and sensors increased the leaked energy amplitude decreased, as expected. The amplitude values decrease substantially after 36 inches and renders the rest of the readings *potentially* too small for monitoring for changes over time. A signal amplifier may be of help in the future to increase the gains. Additionally, as it can be seen in Figure 39 (a), the transmitter is attached close to the intersection of longitudinal and transverse bars, which can potentially attenuate the energy in both directions causing an additional reduction in the coverage distance. Future field studies will attempt to identify locations that are farther from intersections, if possible.

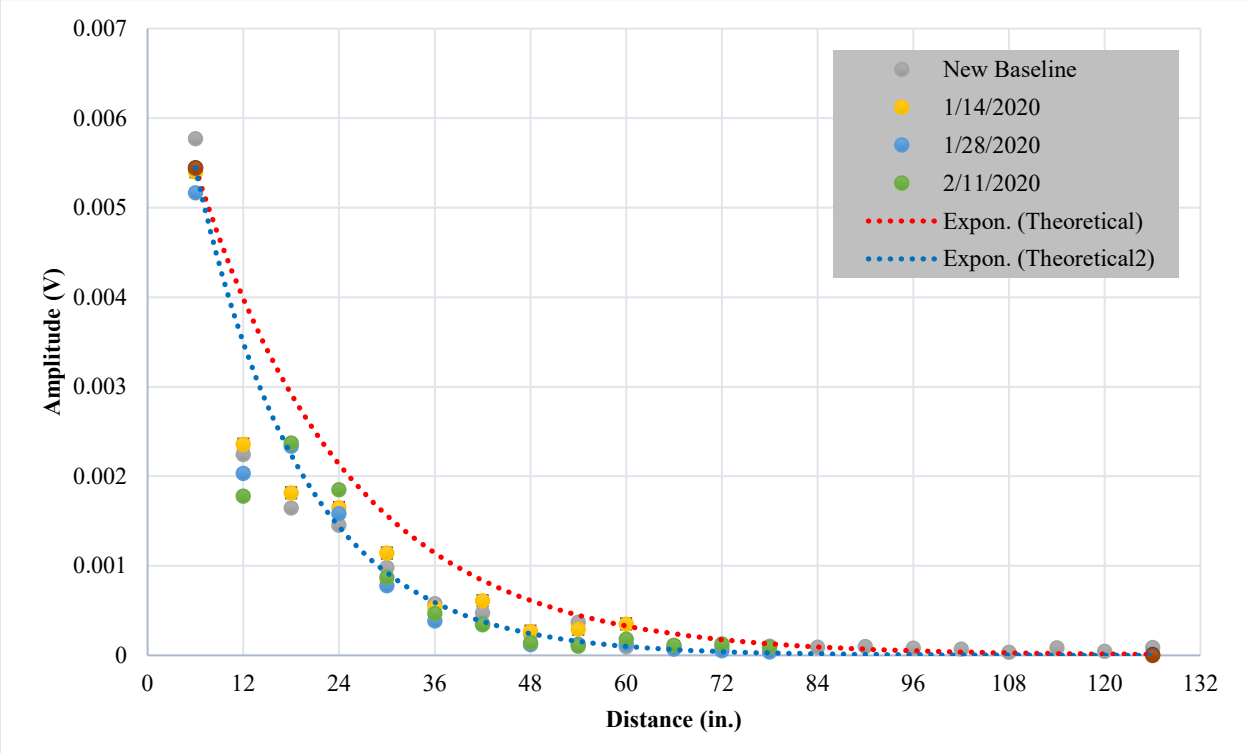

Figure 40. UGWL measurements from Valparaiso Bridge

The Valparaiso bridge will be continuously monitored as a long-term structural health monitoring pilot study, ideally over a few years and/or until a significant change occurs, whichever comes first. While short-term deterioration is not expected in this brand-new bridge cast with epoxy-coated bars, the data will prove useful for all future steps related to the development of this method. In the future, the researchers hope to instrument an additional site, ideally a deck patching project on an older bridge,

where some deterioration may be inherent or happen sooner, and the method can be used to inform the progression of deterioration and durability of such repair projects.

5. Conclusions

This report presents the latest advancements on a novel ultrasonic structural health monitoring technique based on the ultrasonic guided wave theory. The method uses the steel reinforcing rebar as a wave guide and measures the leaked energy from the concrete surface with an array of sensors, and is named ultrasonic guided wave leakage method, or UGWL method. The experimental study presented in this report demonstrates the improvements in the feasibility and reliability of the proposed UGWL method. Further, it is shown that the method provides an attractive alternative to the commonly used half-cell potential method for corrosion detection and monitoring. Based on the experimental work presented in this report, the following specific conclusions can be made:

1. The experimental results showed that Ultragel II has some minor advantages over White Lithium Grease, but both materials can be effectively used for coupling the sensors to the surface.
2. Hydrocal gypsum is a fast and effective material to attach the transmitter on a rebar. It can be molded easily to different angles with a pre-made mold, therefore it allows for an angled and embedded attachment. The attachment should be wrapped in weather-proof material, such as duct-tape, before the surrounding concrete is poured.
3. Optimal angle of attachment is between 0 and 33-degrees from vertical. Future specimens with 15-degrees will be tested and results will be disseminated in technical documents such as research papers.
4. Specimen Set 1 results suggest that 50% change in amplitude of UGWL may be the threshold for a “significant change” in the condition of reinforced concrete systems.
5. Specimen Set 1 results also point out that significant changes in UGWL data started as early as 9 days for the lab specimens submerged in 10% NaCl. Within 175 days, the change in UGWL amplitudes were as high as 154% with respect to the baseline. The 154% increase in UGWL amplitude change correlated to a 0.84% Chloride content, which is 420% over the 0.2% chloride threshold defined by ASTM 1152. ***This finding shows a strong potential for the proposed UGWL method for corrosion monitoring***, because even at 0.2% Chloride content by cement weight (*i.e.* at the ASTM 1152 threshold), the UGWL readings presented a 40% increase in amplitude.
6. Specimen Set 1 results also indicate that when UGWL and HCP are benchmarked, most of the data was in good agreement. UGWL data showed significant change in amplitudes, even when HCP data resulted in the “uncertain” designation. As such, UGWL may be able to detect corrosion activity sooner than HCP.
7. Several other advantages of UGWL over HCP in addition to earlier detection are identified, including the fact that HCP is limited to use with black bars only, while UGWL can be used on epoxy-coated bars.
8. The embedded transmitter installation at the Valparaiso Bridge was successful. It was observed that the first 3 feet provide the best range, but data can be collected at distances of up to 14 feet. It should be noted that in this case, the transmitter was not mounted on an angle, therefore there was no direction to the wave. In other words, this translates into a 28 feet of data collection with a single transmitter. Data has been monitored for over a month thus far, and monitoring will resume after labs reopen and past the conclusion of this particular project. No significant change is expected immediately, but a continuous and large data pool will be

crucial in further developing the method, confirming the durability of the embedment, and to verify the success of the method in the long term. The lessons learned from the experimental study suggest that the sensor should be attached away from the intersection of bars, and an angled attachment and amplifier can improve signal magnitudes.

9. For optimal grid for the sensors on the bridge decks, it is recommended to align the receiver array on top of the rebar with the transmitter, and take readings every 6 inches up to 14 feet. In heavily reinforced concrete decks, each array will likely only serve to monitor flaws in/around that rebar with acceptable statistical confidence.
   In terms of the feasible distance that can be scanned along the rebar, while previous work (Erdogmus et al., 2020) shows that data legible readings of the leaked energy can be obtained up to 14 ft; the exponential attenuation of the energy makes it difficult to note relatively changes in amplitude at these smaller magnitudes. Considering the bidirectional and multi layered reinforcement and other complexities of real-world situations, a more reasonable distance for the scan range is 3 feet. Scan length limitations of this method are similar to those with other NDT methods. For instance, the success of the ground penetrating radar (GPR) scan lengths and grid resolution is directly related to the depth and size of the object investigated underground as well as the frequency of the antenna.

In the future, it is suggested that to scan larger areas, multiple sensors should be embedded and baseline readings should be correlated. In addition, use of an angled attachment to the rebar will be investigated as this can help increase the amount of energy directed parallel to the wave guide (rebar) and therefore improve upon this initially suggested scan distance (3 ft). Finally, better sensors (than currently available in the industry in terms of size and shape) manufactured in response to the development of this novel method and use of signal amplifiers can help improve the scanning distance and range of applications for the proposed method.

6. Acknowledgments

This research was funded by the Nebraska Department of Transportation (NDOT). The research team would like to thank the NDOT Technical Advisory Committee members for their valuable feedback throughout the project. The authors also present their deepest gratitude to various undergraduate researchers who contributed in this research program: Kelsey Stithem, Monica Houck, Mitchael Sieh, Dylan Thompson, Ben Schnatz, and Uziel Ramos. The Chemistry Department at the University of Nebraska is acknowledged for their assistance in the chloride testing. Authors also thank the assistance of UNL's lab manager Peter Hilsabeck and lab technician Jose Lopez who were of great assistance during the specimen casting and coring processes.

7. References

ACI Committee 357. (1984). 357R-84: Guide for the Design and Construction of Fixed Offshore Concrete Structures (Reapproved 1997). *Technical Documents*.

Angst, U., Elsener, B., Larsen, C. K., & Vennesland, Ø. (2009). Critical chloride content in reinforced concrete—A review. *Cement and Concrete Research*, *39*(12), 1122–1138.

Ann, K. Y., & Song, H.-W. (2007). Chloride threshold level for corrosion of steel in concrete. *Corrosion Science*, *49*(11), 4113–4133.

ASTM, C. (1999). 876-99 Standard, Test method for half-cell potentials of uncoated reinforcing steel in concrete. *West Conshohocken, PA, ASTM International*.

ASTM, C. (2012). *Standard test method for acid-soluble chloride in mortar and concrete*. *West Conshohocken, PA, ASTM International*.

Cui, J. (2012). *Multiple Sensor Periodic Nondestructive Evaluation on Concrete Bridge Deck Maintenance*. University of Vermont.

Garcia, E., Erdogmus, E., Schuller, M., & Harvey, D. (2017). Novel Method for the Detection of Onset of Delamination in Reinforced Concrete Bridge Decks. *Journal of Performance of Constructed Facilities*, *31*(6), 04017102.

Garcia, Eric, Erdogmus, E., Schuller, M., & Harvey, D. (2019). Detecting Onset of Different Types of Flaws in Reinforced Concrete. *ACI Materials Journal*, *116*(1).

Glass, G. K., & Buenfeld, N. R. (2000). Chloride-induced corrosion of steel in concrete. *Progress in Structural Engineering and Materials*, *2*(4), 448–458.

Hartt, W. H., Powers, R. G., Leroux, V., & Lysogorski, D. K. (2004). *Critical literature review of high-performance corrosion reinforcements in concrete bridge applications*. United States. Federal Highway Administration Publication Number FGWA-HRT-4-093. Office of Infrastructure R&D, McLean, Virginia.

NRMCA | TiPs: Technology in Practice. (n.d.). Retrieved February 9, 2020, from https://www.nrmca.org/aboutconcrete/tips/default.asp

Rose, J.L. (1999) Ultrasonic Waves in Solid Media. Cambridge University Press, Cambridge. - References—Scientific Research Publishing. (n.d.). Retrieved May 21, 2019, from

https://www.scirp.org/(S(vtj3fa45qm1ean45vvffcz55))/reference/ReferencesPapers.aspx?ReferenceID=1896876

Standard, B. (1997). *Structural Use of Concrete: Code of Practice for Design and Construction, Part 1, BS 8110*. British Standard Institution, UK.

TIP (2020). *Technology in Practice: What, Why & How?*, National Ready Mix Concrete Association (NRMCA). Website: https://www.nrmca.org/aboutconcrete/tips/default.asp. Last accessed 6/11/2020

Yunovich, M., Thompson, N. G., Balvanyos, T., & Lave, L. (2001). Corrosion cost and preventive strategies in the United States—Appendix D—highway bridges. *Federal Highway Administration, FHWA-RD-01*, *157*.

8. Appendix: Photos from Valparaiso Bridge (S066-06060) Instrumentation

Installation Day Images (10-14-2019)

Concrete Pour Day Images (10-15-2019)

Post-Concrete Pour Image (04-07-2020)